PHYSICAL REVIEW LETTERS

VOLUME 3 JULY 15, 1959 NUMBER 2

CALCULATION OF PARTITION FUNCTIONS*

J. Hubbard†
Department of Physics, University of California, Berkeley, California
(Received June 15, 1959)

It is the purpose of this Letter to describe briefly the manner in which a transformation due to Stratonovich[1] can be used to calculate approximately the grand partition functions of some many-body systems.

Consider the grand partition function

$$Z = \mathrm{Tr}[\exp(-\beta K - \beta V - \nu N)],$$

where

$$K = \sum_i \epsilon_i \eta_i^* \eta_i, \quad V = \tfrac{1}{2} \sum_{i,j,k,l} v_{ij;kl} \eta_i^* \eta_j \eta_k^* \eta_l,$$

$$N = \sum_i \eta_i^* \eta_i, \quad \beta = 1/\kappa T, \quad \nu = \mu/\kappa T,$$

(T = temperature, μ = chemical potential) and the η_i^* and η_i are the creation and destruction operators for the particles of the system; the η_i^* and η_i may have commutation relations appropriate to either Bose-Einstein or Fermi-Dirac statistics.

It should be noted that $v_{ij;kl} = v_{kl;ij}$ necessarily, so that V can be regarded as a quadratic form in the variables $\xi_{ij} = \eta_i^* \eta_j$. Bringing this quadratic form into normal form one has $V = \sum_\alpha \lambda_\alpha \rho_\alpha^2$, where the λ_α are real and the ρ_α are linear combinations of the ξ_{ij}. The grand partition function may now be rewritten

$$Z = \mathrm{Tr}[\exp(-\beta K - \nu N - \beta \textstyle\sum_\alpha \lambda_\alpha \rho_\alpha^2)]. \qquad (1)$$

One can now transform this expression by making use of the identity

$$\int_{-\infty}^{\infty} \exp\{-\pi x^2 - 2\pi^{1/2} a x\}\, dx = \exp\{a^2\}. \qquad (2)$$

This identity cannot be applied directly to (1) because of the noncommutativity of the operators involved. To overcome this difficulty one may make use of the ordering label technique of Feynman[2] and introduce an ordering label s to write

$$Z = \mathrm{Tr}\{\exp[-\textstyle\sum_s (K_s + \mu N_s) - \sum_\alpha \sum_s \lambda_\alpha \rho_{\alpha s}^2]\}, \qquad (3)$$

where $\sum_s$ has been written for $\int_0^\beta ds$; the quantities in (3) can now be handled as though they were c numbers, the ordering determined by s being restored when convenient.

Applying the identity (2) to (3) one now easily finds

$$Z = \int \exp\{-L[x_{\alpha s}]\} \prod_{\alpha s} dx_{\alpha s}, \qquad (4)$$

where

$$L[x_{\alpha s}] = \pi \sum_{\alpha, s} x_{\alpha s}^2 + \beta f[x_{\alpha s}], \qquad (5)$$

and

$$\exp\{-\beta f[x_{\alpha s}]\} = \mathrm{Tr}\left\{\exp\left[-\sum_s (K_s + \mu N_s) - 2\pi^{1/2} \sum_{\alpha s} (-\lambda_\alpha)^{1/2} x_{\alpha s} \rho_{\alpha s}\right]\right\}. \qquad (6)$$

The essential feature of the transformation (4)-(6) is that the operator appearing in the exponent in (6) is only quadratic in the operators η_i^*, η_i, so that the evaluation of the indicated trace is essentially similar to the evaluation of the partition function of a system of noninteract-

Copyright 1959 by the
American Physical Society

ing particles moving in a field determined by the $x_{\alpha s}$. Equations (4) and (5) then express Z as a weighted average of the quantity (6) over the fields $[x_{\alpha s}]$.

In some cases the integral (4) can be conveniently evaluated by the method of steepest descents. One then finds

$$\ln Z \approx -\pi\sum_{\alpha}(x_{\alpha}{}^{0})^{2} - \beta f[x_{\alpha}{}^{0}] - \tfrac{1}{2}\ln[\det(L_{2})_{0}], \quad (7)$$

where the $x_{\alpha}{}^{0}$ are determined by the equation

$$(\partial L/\partial x_{\alpha s})_{0} = 0 \quad (8)$$

(it can be shown that the solution $x_{\alpha s}{}^{0}$ of this equation is independent of s, hence the use of the abbreviated notation $x_{\alpha}{}^{0}$ for $x_{\alpha s}{}^{0}$), while L_2 is the matrix

$$(L_{2})_{\alpha s;\gamma s'} = \frac{1}{2\pi}\frac{\partial^{2}L}{\partial x_{\alpha s}\,\partial x_{\gamma s'}}; \quad (9)$$

$(\ )_0$ means that the quantity is evaluated at $x_{\alpha s} = x_{\alpha}{}^{0}$.

Evaluation of the formulas (7)-(9) shows that (8) represents an obvious generalization to finite temperature of the ordinary Hartree self-consistent-field equations, while the first two terms of (7) represent the energy in the Hartree approximation and the last term of (7) is (at $T=0$) essentially the correlation energy calculated in the approximation of Brueckner and Gell-Mann.[3]

We add a few remarks concerning some of the features and the range of application of the method illustrated above.

(*i*) In a higher approximation Eq. (8) determining $x_{\alpha}{}^{0}$ is replaced by

$$\left[\frac{\partial}{\partial x_{\alpha s}}\left\{L[x_{\alpha s}] + \tfrac{1}{2}\ln\det(L_{2})\right\}\right]_{0} = 0. \quad (10)$$

This equation represents a generalization of the Hartree-Fock equations to include the effects of correlation in the approximation of Brueckner and Gell-Mann.[3]

(*ii*) It is possible to write V as a Hermitean form in the variables $\zeta_{ij} = \eta_i\eta_j$. Writing V in this form and proceeding in the same manner as above, one obtains results formally similar to those given above but representing a different method of approximation in the calculation of Z.

(*iii*) In the approximation described in (*ii*) the equation equivalent to (8) no longer represents the Hartree-Fock equations, but in the Fermi-Dirac case constitutes a set of equations which are generalizations of (and include) the Bardeen, Cooper, and Schrieffer equations of superconductivity.[4]

(*iv*) In the approximation described in (*ii*) the term equivalent to the last term of (7) represents (at $T=0$) the correlation energy calculated in the approximation of the Brueckner nuclear matter theory.[5]

(*v*) In the approximation described in (*ii*), the equation equivalent to (10) determines at $T=0$ a self-consistent field dependent upon the reaction matrix, of the type introduced in the Brueckner nuclear-matter theory.[5]

(*vi*) In some cases the solutions of (8) are degenerate in the sense that there is a continuum of solutions $x_{\alpha}{}^{0}$ all yielding the same value for $L[x_{\alpha}{}^{0}]$. In this case special measures have to be taken in the application of the method of steepest descents. This situation corresponds physically to the presence of collective motions of the type illustrated by the rotational collective motion of nuclei.

(*vii*) In some cases there may be two or more solutions of (8) representing local minima of L. In evaluating (7) one must of course use the solution $x_{\alpha}{}^{0}$ which makes L an absolute minimum. However, it may be that as β is varied the local minima change their relative positions and the absolute minimum switches at some temperature from one to another local minimum. This process presumably gives a description of some sorts of phase transition.

These remarks will be enlarged upon in a series of papers now being prepared for publication.

---

*This work has been supported in part by the National Science Foundation.

†On leave from the United Kingdom Atomic Energy Authority Research Group, Harwell.

[1]R. L. Stratonovich, Doklady Akad. Nauk S.S.S.R. 115, 1097 (1957) [translation: Soviet Phys. Doklady 2, 416 (1958)].

[2]R. P. Feynman, Phys. Rev. 84, 108 (1951).

[3]K. A. Brueckner and M. Gell-Mann, Phys. Rev. 106, 364 (1957).

[4]Bardeen, Cooper, and Schrieffer, Phys. Rev. 108, 1175 (1957).

[5]K. A. Brueckner, Phys. Rev. 96, 908 (1954); 97, 1353 (1955).

SHORT-TIME MEASUREMENT OF TIME DILATION IN AN EARTH SATELLITE*

R. S. Badessa, R. L. Kent, and J. C. Nowell
Research Laboratory of Electronics, Massachusetts Institute of Technology, Cambridge, Massachusetts
(Received May 25, 1959)

The purpose of this note is to describe a method for measuring the gravitational red shift postulated by Einstein's general theory of relativity. As popularly envisioned, this effect causes clocks at different gravitational potentials to run at different rates.[1] The greatest difference obtainable in the vicinity of the earth, however, is only a few parts in 10^{10}. Nevertheless, measurements of gravitational red shift now appear to be feasible. Atomic clocks with stability approaching 1 part in 10^{11} have been developed, and earth satellites capable of orbiting at altitudes which provide a significant difference in gravitational potential with respect to the earth are available. The method to be described here is basically a short-time-measurement version of a proposed experiment[2,3] involving comparison of the time kept by a stable clock in a satellite and an identical one on the ground. By "short-time measurement" we refer to the interval required to permit the small rate difference of the two clocks (or the frequency difference of two stable oscillators) to accumulate a measurable difference in time (or phase). In previously suggested experiments the required measurement interval has been estimated to be several days or even weeks. In the system described in this note the interval may be as short as 30 seconds or less.

A short-time measurement of gravitational frequency shift offers the following significant advantages:

1. With elliptical orbits, frequency differences can be observed at various radii, to obtain the variation of frequency shift with gravitational potential.

2. If the measurement is repeated when the satellite is at a particular radius (as at perigee), a slow frequency drift between satellite and earth clocks can be determined and removed. Since the quantity of interest is the variation of frequency difference as a function of altitude, a fixed set between clocks is inconsequential. Therefore, quartz crystal oscillators can probably be employed.

3. Continuous integration or counting over many orbital periods is not required. Skipped cycles or temporary failures would not invalidate the experimental results.

The instantaneous frequency difference between an oscillator on the earth and an oscillator on a satellite as received on the earth is influenced by the variation in path length (first-order Doppler). Since this is typically of the order of 1 part in 10^5, and the gravitational shift is of the order of a few parts in 10^{10}, a short-time measurement of gravitational shift utilizing one-way propagation would require extremely accurate knowledge of the path length. A technique for avoiding this difficulty is to transmit to the ground from the satellite a signal which has been "precorrected" in frequency by the increment required to cancel the first-order Doppler shift. For the following step-by-step description of such a system, a point of observation is selected at an earth pole (O in Fig. 1) in order to present a simple analysis that adequately illustrates the principles of measurement.

1. A transmitter of frequency f is on the earth and transmits to the satellite.

2. From the theory of relativity, it can be shown that the frequency of the signal received at the satellite, as observed on the satellite, is

$$f' \approx f(1-\beta\cos\alpha)/(1-\beta^2+2\phi)^{\frac{1}{2}}, \qquad (1)$$

where β is the magnitude of the satellite velocity at the instant of reception, normalized in terms of the velocity of light; α is the angle (measured in the coordinate system of an observer at O)

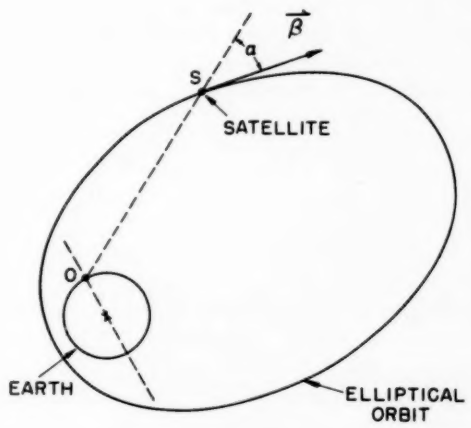

FIG. 1. Geometry of the measurement problem.

between the propagation path O-S and the velocity vector β; ϕ is the difference in gravitational potential (positive) between points S and O, normalized in terms of the square of the velocity of light.

3. The satellite contains an oscillator of frequency $2f$ (measured on the satellite). The received signal frequency f' is subtracted from $2f$ by mixing within the satellite to yield a frequency difference

$$f'' = 2f - f'. \tag{2}$$

4. The mixture signal f'' is transmitted back to the earth. (Reception and retransmission at the satellite are assumed to be virtually instantaneous.) When received, it has a frequency f''', where[4]

$$f''' \approx f''(1-\beta^2+2\phi)^{\frac{1}{2}}/(1+\beta\cos\alpha). \tag{3}$$

Substitution for f'' yields

$$f''' \approx f\left[2-\frac{1-\beta\cos\alpha}{(1-\beta^2+2\phi)^{1/2}}\right]\left[\frac{(1-\beta^2+2\phi)^{1/2}}{1+\beta\cos\alpha}\right]. \tag{4}$$

By means of a power series expansion, retaining second-order terms in β and first-order terms in ϕ, we obtain

$$f''' \approx f(1+2\phi-\beta^2). \tag{5}$$

Note that the first-order Doppler term has been canceled.[5] The received signal frequency differs from the ground transmitter frequency by

$$\Delta f \approx f(2\phi-\beta^2). \tag{6}$$

The two terms contributing to the frequency difference are apparently inseparable experimentally. The first, 2ϕ, stems from a "speeding-up" of time in the satellite as a result of the difference in gravitational potential, i.e., the "gravitational red shift." The second term, $-\beta^2$, known as a second-order Doppler shift, denotes a "slowing-down" of time in the satellite as a result of its orbital velocity. This term, which has been verified experimentally, can be calculated easily, once the orbit of the satellite is known. Subtraction of the calculated second-order Doppler term from the measured frequency difference yields the desired gravitational shift. If the transmitter operating frequency is 500 Mc/sec, the largest expected frequency difference attributable to gravitational shift will be approximately 0.5 cps. This frequency can be determined within ± 0.01 cps by measuring the accumulated phase difference in a 10-second interval to an accuracy of $\pm 36°$.

The authors would like to acknowledge the assistance given by V. J. Bates, J. W. Graham, and Professor C. L. Searle. They would also like to express their appreciation for the invaluable guidance of Professor J. R. Zacharias and Professor G. G. Harvey.

---

*This work was supported in part by the U. S. Army (Signal Corps), the U. S. Air Force (Office of Scientific Research, Air Research and Development Command), and the U. S. Navy (Office of Naval Research).

[1]Lorentz, Einstein, Minkowski, and Weyl, The Principle of Relativity (Reprint, Dover Publications, Inc., New York, 1958): A. Einstein, pp. 37-59, 97-107.

[2]S. F. Singer, Phys. Rev. 104, 1 (1956).

[3]L. H. Aller, Astron. J. 64, 45 (1959).

[4]Equations (1) and (3) are alternative forms for expressing relativistic Doppler shift. The change of form is employed so that only one angle, α, need be considered. The expressions are estimated to be accurate to about 1 part in 10^{14} for the case of interest.

[5]The frequency computed is determined by the values of β and ϕ at a single instant (viz., the instant of reception and retransmission at the satellite). Therefore, the fact that β and ϕ are changing cannot result in an error in first-order Doppler cancellation.

EFFECTS OF 9.2-kMc/sec ULTRASONICS ON ELECTRON SPIN RESONANCES IN QUARTZ

E. H. Jacobsen, N. S. Shiren, and E. B. Tucker
General Electric Research Laboratory, Schenectady, New York
(Received June 16, 1959)

We have observed the reduction in amplitude of electron spin resonances at 9.2 kMc/sec caused by ultrasonic vibrations in the same frequency range. Measurements were made on resonances due to manganese impurity in quartz crystals[1] and also on those due to radiation-induced centers in quartz. The paramagnetic resonance signal from the spins at one end of a quartz crystal was observed as a function of the power and frequency of the ultrasonic vibrations introduced at the other end, and as a function of the monitoring microwave power.

The apparatus utilizes ultrasonic techniques, which have been reported recently,[2,3] together with a standard microwave electron paramagnetic resonance spectrometer using field modulation and synchronous detection. A quartz crystal, in the form of a cylindrical rod 0.3 cm in diameter and 3 cm long, extends between two cavity resonators in a geometry similar to that used in a previous experiment.[4] The spin resonances are observed in a full-wave rectangular cavity with the microwave magnetic field perpendicular to the rod axis. Sound waves are generated at the other end of the rod in a tunable ultrasonic drive cavity of the type used by Bömmel and Dransfeld.[5] The vibrations then travel the length of the bar and interact with the spins in the spectrometer cavity. Experiments were carried out in the temperature range of 1.5 to 2.0°K.

Lines due to manganese in both X-cut and Y-cut quartz have been investigated. The paramagnetic centers were distributed throughout the length of the bar. Two gross effects can be noted in Fig. 1. With constant spectrometer power, the spin-resonance signal amplitude decreases with increasing ultrasonic drive power. The second effect of the ultrasonic power is the shift of the peak of the microwave saturation curve. Increasing the ultrasonic power moves the peak toward higher spectrometer powers. Both effects are to be expected on the basis of simple theory with the ultrasonic vibrations considered as equivalent to a second microwave field (not coherent with the spectrometer field).

By varying the ultrasonic frequency while keeping the spectrometer frequency constant we can, in principle, determine the bandwidth for the interaction of the vibrations with a particular resonance line. A typical result for one of the manganese lines is given in Fig. 2. The ultrasonic width differs from line to line and seems to be smaller than the observed microwave linewidth for the same line.

The narrow bandwidth observed for the interaction of the vibrations with the Mn spins rules out thermal heating of the quartz bar by the

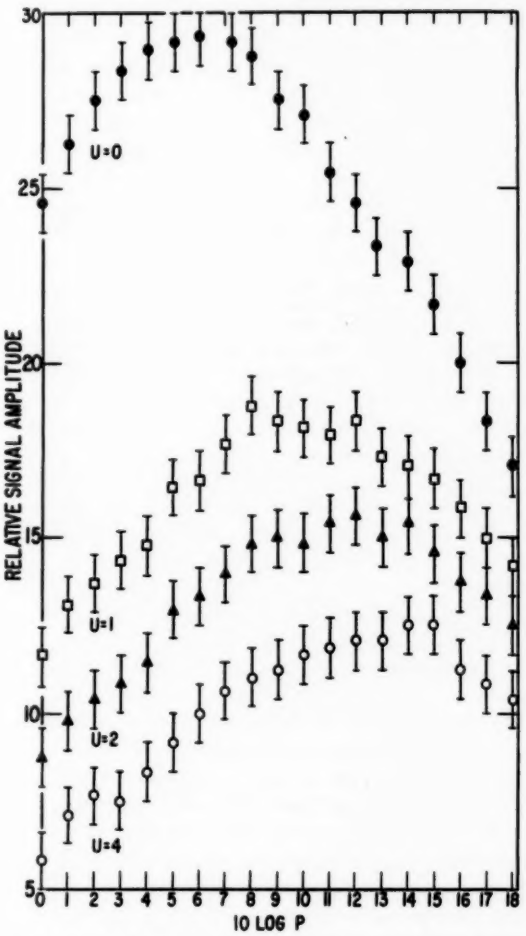

FIG. 1. Derivative of absorption as a function of the logarithm of spectrometer power (P) for several relative values of ultrasonic power (U) for a line due to manganese in quartz. Spectrometer and ultrasonic frequencies are identical to within a few kc/sec.

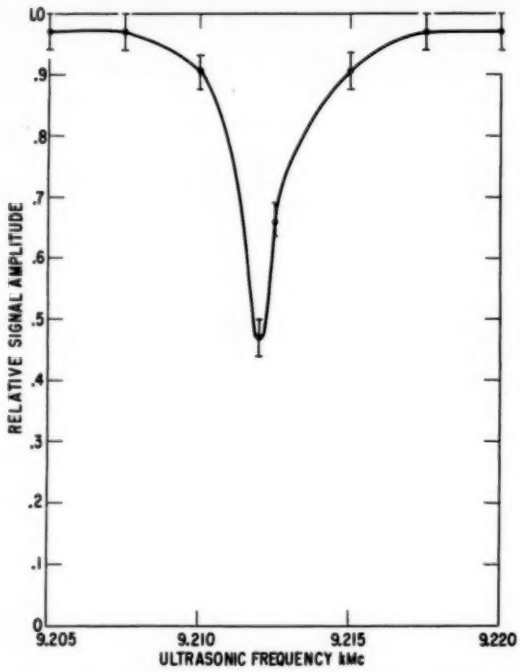

FIG. 2. Amplitude of derivative of absorption as a function of ultrasonic frequency with constant spectrometer frequency, magnet field, ultrasonic power, and spectrometer power. The data are for the same line of Mn in quartz as the data of Fig. 1.

ultrasonic energy or by dielectric heating in the drive cavity as the agent producing the effect. Electromagnetic feed-through is also ruled out as a cause of the effect by observing that the power in the ultrasonic drive cavity has no effect on the resonance signal if the quartz rod is broken or cut at a point between the two cavities.

The dependence of the signal on the ultrasonic power for manganese resonances in quartz cannot be expressed by a simple functional relationship, and in fact, is not the same for all the lines observed. This is not unexpected, since all the observed lines saturated with spectrometer power in a way which indicates partial inhomogeneous broadening[6] and the relationship between signal amplitude and ultrasonic drive power is affected by inhomogeneous broadening as well as by nonuniformity of the ultrasonic field.[7] These same factors will affect the relation between the observed vibration-spin bandwidth (Fig. 2) and the true vibration-spin bandwidth. This true bandwidth is expected to be the homogeneous width of the resonance line.

The narrow line observed for the vibration-spin interaction in the Mn case is evidence against the spreading of the phonon modes in the immediate vicinity of the ultrasonic frequency.

The effect of the microwave phonons on the "smoky quartz" resonance centers[5,9] induced by electron, neutron,[10] or x irradiation is rather different. The neutron-induced centers, like the Mn, extended through the whole length of the bar whereas the electron- and x-ray-induced centers were generated only in that part of the bar used in the spectrometer cavity. As before, increasing the ultrasonic power decreases the signal amplitude, but in contrast with the Mn, the observed bandwidth is greater than our tuning range of ±500 Mc/sec.

In an attempt to understand the bandwidth of over 1000 Mc/sec for the vibration-spin interaction in the radiation-induced centers, we have carried out pure piezoelectric-acoustic experiments[1,3,4] on the same quartz bars. The results showed that the X-cut bars of the irradiated quartz give more echoes than X-cut bars containing manganese. This seems to eliminate the possibility of a broad phonon band being responsible for the large bandwidth. It has been impossible to obtain piezoelectric-acoustic measurements on Y-cut crystals because of coherence problems due to coupling to other modes.

In all of the vibration-spin interaction experiments it was found that a longitudinal ultrasonic wave (axis of the bar parallel to x axis of the crystal) produces an effect similar to that caused by predominantly transverse waves (axis of the bar parallel to the quartz y axis).

It is a pleasure to acknowledge numerous discussions with Dr. W. Känzig and Dr. T. G. Castner. T. G. Kazyaka helped take most of the data.

---

[1]The spin Hamiltonian of the manganese in quartz system is not yet known.

[2]H. E. Bömmel and K. Dransfeld, Phys. Rev. Letters 1, 234 (1958).

[3]E. H. Jacobsen, Phys. Rev. Letters 2, 249 (1959).

[4]N. S. Shiren and E. B. Tucker, Phys. Rev. Letters 2, 206 (1959).

[5]H. E. Bömmel and K. Dransfeld, Phys. Rev. Letters 2, 298 (1959).

[6]T. G. Castner, Jr., Bull. Am. Phys. Soc. 4, 21 (1959), and Phys. Rev. (to be published).

[7]In the case of ultrasonic vibrations interacting with nuclear spins, effects attributed to standing waves have been reported by Jennings, Tanttila, and Kraus, Phys.

Rev. 109, 1059 (1958).
[8]Griffiths, Owen, and Ward, Nature 173, 439 (1954).
[9]M. C. O'Brien, Proc. Roy. Soc. (London) A231, 404 (1955).

[10]The neutron irradiation was supervised by Dr. R. A. Weeks, at Oak Ridge National Laboratory.

EXCITATION OF HYPERSONIC WAVES BY FERROMAGNETIC RESONANCE

H. Bömmel and K. Dransfeld
Bell Telephone Laboratories, Murray Hill, New Jersey
(Received June 18, 1959)

We have observed the emission of transverse hypersonic waves from a Ni film, deposited on a quartz surface and excited to ferromagnetic resonance. The acoustic frequency was equal to the ferromagnetic resonance frequency. The Ni film, about 18.000 A thick, was evaporated in vacuo on to one end face of a cylindrical single-crystalline quartz rod of 3-mm diameter and 12 mm long. Both end faces of the rod were polished optically flat and parallel. The rod was an oriented *AC*-cut crystal so as to allow the transmission and detection of transverse sound waves.[1] As shown in Fig. 1, the quartz rod was with its two ends part of two cavities C_1 and C_2. One side carrying the Ni film was in the cavity C_1 exposed to an rf magnetic field parallel to the Ni surface, while the other side of the rod was in the electric field of cavity C_2. Both cavities were tuned to the same frequency of 1000 Mc/sec. C_1 was coupled to a pulsed rf generator and C_2 to a receiver and scope. A variable dc magnetic field was applied parallel to the rod axis.

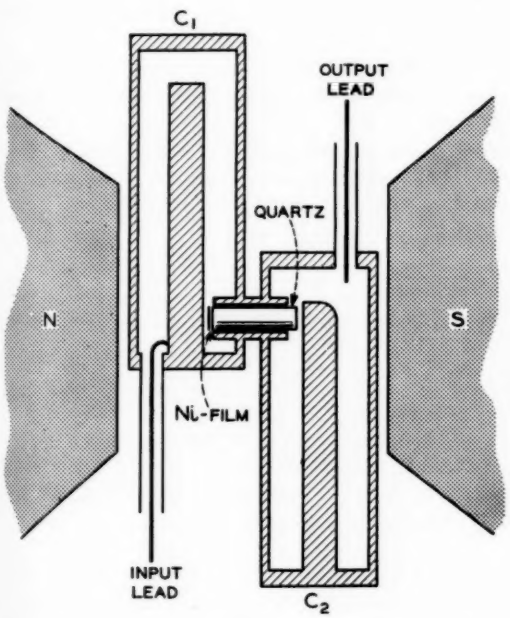

FIG. 1. Experimental arrangement for detection of hypersonic waves, generated by a Ni film in ferromagnetic resonance.

Acoustic waves emitted from the Ni film into the quartz rod were received in cavity C_2. The received power is plotted vs the magnetic field in Fig. 2. The maximum acoustic power of about 1 mw was emitted at a field at which ferromagnetic resonance was observed simultaneously in cavity C_1. A small subsidiary line is visible at fields below the saturation magnetization of 6100 gauss. The acoustic character of the received signal was evident from the delay time between the power pulse sent into cavity C_1 and the received signal from C_2, corresponding to the acoustic delay in the quartz rod. Since the rod has *AC* orientation, the received acoustic waves were of transverse polarization.

We have also observed that, with the same efficiency, ferromagnetic resonance can be excited by incident hypersonic waves: A signal of the same magnitude could be seen, if the roles of the two cavities were exchanged, putting now power into cavity C_2 and receiving from C_1. In this case transverse hypersonic waves were ex-

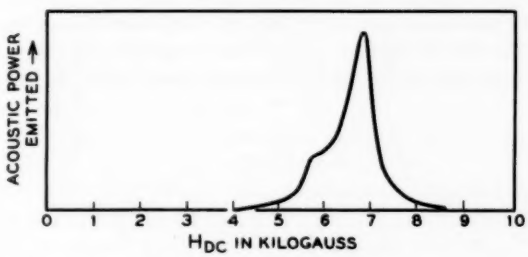

FIG. 2. Magnetic field dependence of hypersonic power emitted from Ni film.

cited in C_2 and the Ni film served as an acoustic receiver. In both experiments the orientation of the dc magnetic field for maximum signal was found to be critical within one degree.

A uniform precession of the magnetization in the film is related, by magnetostriction, to a stress ellipsoid also precessing around the dc magnetic field. If the direction of the dc field is normal to the film it can be shown that, at ferromagnetic resonance, the surface will undergo a rotational shear motion around the dc field, and the film will therefore emit circularly polarized transverse sound waves into the quartz, on which it is plated. Since the film, used here, was not much thicker than half an acoustic wavelength, the shear strain is approximately uniform over the sample. Assuming further that the film is acoustically matched to the quartz, the acoustic power emitted from the film should be of the order

$$P = \rho V_{tr}^{3} \lambda^{2} \varphi^{2}, \qquad (1)$$

where ρ = density of Ni, V_{tr}^{3} = transverse sound velocity in Ni, λ = magnetostriction constant, and φ = precession angle. According to this estimate, the observed maximum power output of about 1 mw could be accounted for by a precession angle of 0.2°, under the assumption that the magnetostriction λ is at these frequencies the same as in static experiments. It may be mentioned, that for other orientations of the dc magnetic field it should also be possible to excite sound waves of twice the frequency of the ferromagnetic resonance.

It is interesting to consider also the case that the film is thicker than the acoustic wavelength, but not exceeding the penetration depth, by using for example a thicker ferrite disk. When such a sample is excited to a uniform spin precession, the corresponding magnetostrictive stress will also be uniform and a displacement can, initially, only take place at the surface. Similarly to the piezoelectric case,[1] elastic waves are therefore excited at the surface. For a uniform precession (precession angle φ) acoustic power is emitted from the surface according to (1), if standing waves and reflections are neglected.

If the spin precession is not uniform, acoustic waves can also be excited by spin waves as treated, for example, by Kaganov et al. and by Kittel.[2] Although the spin wave excitation is quite different from the surface excitation for large samples, there is little distinction between both processes if the sample is thinner than an acoustic wavelength. Kittel[2] suggested that it may be possible to generate acoustic waves by using thin ferrite crystals. The magneto-acoustic resonance in yttrium iron garnet, observed by Spencer and LeCraw,[3] occurred at frequencies orders of magnitude below the ferromagnetic resonance frequency and is therefore a different process. These experiments also demonstrate a new method for the excitation and detection of hypersonic waves, and for their transmission into other solids without bonding them to piezoelectric crystals. The efficiency of this method is, for Ni and at room temperature, not smaller than in the piezoelectric excitation. There should be no difficulty in extending these experiments to higher frequencies or other ferromagnetic materials. For example, we have also observed at 1000 Mc/sec the generation of sound with a much thicker disk of yttrium iron garnet bonded to an AC-cut quartz crystal, between room temperature and 20°K.

We wish to thank J. F. Dillon and E. G. Spencer for interesting discussions and for supplying us with the ferrite samples, A. Grieco and P. Andreatch for making the acoustic bonds, E. M. Kelley for the evaporation of the films and, particularly, A. DiGiovanni for his great help with all the experiments.

---

[1] H. Bömmel and K. Dransfeld, Phys. Rev. Letters 1, 234 (1958); 2, 298 (1959).

[2] N. I. Kaganov and Z. M. Tsukernik, Zhur. Eksptl. i Teoret. Fiz. 36, 224 (1959); C. Kittel, Phys. Rev. 110, 836 (1958).

[3] E. G. Spencer and R. C. LeCraw, Phys. Rev. Letters 1, 241 (1958).

NUCLEAR SPIN RELAXATION TIME IN SUPERCONDUCTING ALUMINUM

Alfred G. Redfield
International Business Machines Watson Laboratory at Columbia University, New York, New York
(Received June 5, 1959)

The nuclear spin relaxation time T_{1S} in superconductors was first measured by Hebel and Slichter[1,2] just below the transition temperature in aluminum, and by Reif[1] well below the transition temperature in mercury. These measurements indicated that T_{1S} decreases rapidly just below T_C, and then rapidly increases again well below the transition temperature, becoming greater than the normal state relaxation time at very low temperatures. Hebel and Slichter pointed out[1] that the decrease in T_1 near T_C could be easily explained only in terms of an energy gap model of superconductivity. They supported their explanation with a detailed calculation[2] based on the Bardeen, Cooper, and Schrieffer (BCS) theory of superconductivity. Comparison of the temperature dependence of T_1 as contrasted with that of acoustic attenuation provides confirmation of the spin-dependent correlation of the wave functions used in the BCS theory.[2]

Preliminary measurements of T_1 in aluminum by Anderson and the writer[3,4] were in reasonable agreement with the Hebel-Slichter-BCS theory; accuracy of these measurements has now been improved using a He^3 cryostat. The experimental method was basically the same as that used previously.[1] The sample was soaked in a 3000-gauss field for a time long compared to T_1, so that the spin magnetization built up to its equilibrium value in this field. The field was then turned off in about 1/10 sec and left off for a variable time τ; during this time the sample is in the superconducting phase and the spin polarization relaxes toward zero. The field is then turned on to 1000 gauss and within 2/10 second the spin polarization is measured in the normal state by applying suitable rf and sweep fields.

The sample was immersed in liquid He^3 to eliminate temperature changes due to the magneto-caloric effect; temperature was inferred from measurement of the magnetic susceptibility of a solid cylinder of iron ammonium alum, with an estimated error of 2%.

The recent data are plotted in Fig. 1, together with earlier data[5] taken in this laboratory, as a function of T_C/T (assuming $T_C = 1.178°K$). The signal to noise ratio was 10 or better, and the signal appeared to decrease exponentially with

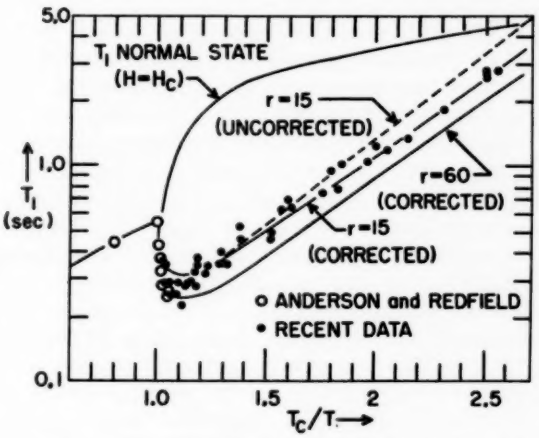

FIG. 1. Experimental and theoretical nuclear spin relaxation time in pure aluminum plotted as a function of inverse reduced temperature.

τ for all the points shown. We do not believe that possible impurities affected the data of Fig. 1, and we are currently attempting to confirm this by studying the effect of known impurity concentrations.

A possible source of error in this experiment is the presence of regions of trapped flux. Such regions would give a contribution to the observed T_1 characteristic of the normal state at $H = H_C$, which might not be resolved with the poor signal to noise ratio in the present experiment. We have plotted in Fig. 1 the semiempirical temperature dependence of T_1 in the normal state at H_C, based on actual measurements at 0.5° and on measurements of T_1 above T_C, as a function of field.[5] Since there is no noticeable correlation between the variation of the normal state T_1 and the superconducting T_1, and since they are very different over much of the range, we believe that the effect of trapped flux is small.

The data of Fig. 1 are in reasonable agreement with the earliest measurements[1] of Hebel and Slichter and of Reif, and are in detailed agreement with the predictions of Hebel and Slichter based on the BCS theory. For comparison we have plotted in Fig. 1 recent calculations of T_{1S} by Hebel,[6] based on the expressions found in

reference 2 but evaluated more accurately. There are two unknown parameters in the theory: a multiplicative constant which is determined by the requirement that T_1 be continuous at the critical temperature, and a parameter $r=\epsilon_0(0)/\Delta$, where $\epsilon_0(0)$ is the half gap width of BCS at 0°K ($3.5kT_c$) and Δ can be regarded as the half-width of the electronic energy levels. In reference 2, Δ is introduced into the theory by smearing or folding the BCS density of states function with a square function of width 2Δ and height $(2\Delta)^{-1}$. Δ can be interpreted either as an uncertainty width due to electron scattering mechanisms not accounted for in the BCS theory, or as a smearing of the BCS density of states due to anisotropy of the energy gap.[7]

The "uncorrected" curve in Fig. 1 is that calculated by Hebel directly from the BCS theory for $r=15$; for other values of r the curve is nearly parallel to this one for $T_c/T>1.5$. The "corrected" curves are calculated using the energy gap found experimentally by Biondi and Garfunkel from microwave measurements[8] [i.e., $\epsilon_0(T)$ proportional to, but 7.5% smaller than, the BCS prediction]. According to Hebel,[6] the calculation of T_{1S} can be corrected for an energy gap different from the BCS prediction if the form of the BCS wave functions is correct, and only their energies are assumed to be incorrect. In that case $T_{1S}T$ is a function of $\epsilon_0(T)/kT$ alone.

Agreement with theory is excellent assuming $r=15$ [$\Delta=\epsilon_0(0)/15$]. This agreement is in contrast with the Knight-shift observations of Reif and of Androes and Knight.[9] Our measurements are made on particles large compared to the coherence length (10^{-3} cm). The parameter Δ is nearly temperature independent, consistent with the idea that it represents either the inverse electronic lifetime against boundary scattering, or more likely anisotropy of the energy gap.[7] It is probable that if Δ represented phonon scattering, it would be strongly temperature dependent, contrary to observation.

It is a pleasure to acknowledge the contribution to this research of Dr. A. G. Anderson, who collaborated on the early measurements. The writer is also indebted to many other members of this laboratory, especially Mr. W. V. Kiselewsky and Dr. H. A. Reich. Finally he wishes to thank Dr. L. C. Hebel and Professor C. P. Slichter for several interesting discussions and for communicating the progress and results of their research prior to publication.

[1]L. C. Hebel and C. P. Slichter, Phys. Rev. 107, 901 (1957).

[2]L. C. Hebel and C. P. Slichter, Phys. Rev. (to be published).

[3]A. G. Anderson and A. G. Redfield, Bull. Am. Phys. Soc. 2, 388 (1957).

[4]A. G. Redfield and A. G. Anderson, Physica 24, S150 (1958).

[5]A. G. Anderson and A. G. Redfield, Proceedings of the Fifth International Conference on Low-Temperature Physics and Chemistry, Madison, Wisconsin, August 30, 1957, edited by J. R. Dillinger (University of Wisconsin Press, Madison, 1958).

[6]L. C. Hebel (to be published). We wish to thank Dr. Hebel for permission to quote his calculations prior to publication.

[7]P. W. Anderson, Bull. Am. Phys. Soc. 4, 148 (1959).

[8]M. A. Biondi and M. P. Garfunkel, Phys. Rev. Letters 2, 143 (1959).

[9]G. M. Androes and W. D. Knight, Phys. Rev. Letters 2, 386 (1959).

OPTICAL MASER DESIGN

J. H. Sanders*
Bell Telephone Laboratories, Murray Hill, New Jersey
(Received June 2, 1959)

Schawlow and Townes[1] have discussed the possibility of operating a maser in the infrared or visible wavelength region. They point out that the difficulty of maintaining an adequate population excess in the upper of the two levels between which maser action takes place increases rapidly with the operating frequency because of the large rate of spontaneous emission. They envisage only the use of photon excitation for populating the appropriate level in the working medium.

In observing the resonance absorption of a spectral line, there exists the well-known difficulty of obtaining a large amount of light from a source without broadening the line to the point where only a fraction of the total is absorbed. In view of this, it appears difficult to employ effi-

ciently optical excitation of a maser working in the visible region. The use of electron impact excitation of the working medium would reduce the practical difficulty of obtaining a sufficient density of excited atoms, and the use of a discharge in the medium itself is suggested. In a medium containing a single gas or vapor, the possibility of obtaining the required excess population in the upper of two levels exists in cases where there is a favorable lifetime ratio, i.e., a long-lived upper state and a short-lived lower state. As an example of this, the 6678A line in helium I is due to a transition between the $3\,^1D_2$ state, mean life 1.5×10^{-8} sec, and the $2\,^1P_1$ state, mean life 4.3×10^{-10} sec. Many processes exist in a discharge which may disturb the relative population of such levels from the value implied by these lifetime values, and it may be possible to choose conditions which maintain a high population in the upper state.

Detection of the onset of continuous oscillation in the optical maser working in the visible region would be particularly simple. The Fabry-Perot étalon, used as the "cavity" of the maser, gives a concentric fringe system at infinity when the light source is placed between the plates, similar to the conventional case when the étalon is used by transmission. Using highly reflecting plates, of which only one need transmit a small percentage of the light, and a spacing of several centimeters, the width of the observed rings would normally be larger than the instrumental width. If maser oscillation were taking place, due to the presence of an adequate excess population in an upper level in the medium between the plates, the light due to this process would have an extremely small frequency width, and lines of the instrumental width would appear superimposed on the broader lines due to spontaneous emission. To confine oscillation to only one order, or mode, the aperture of the étalon could be restricted to reduce the number of effective beams in those orders in which the light is not normal to the plates. The order in which maser oscillation would be most likely to occur would then be the central, or normal, order.

---

*On leave from the Clarendon Laboratory, Oxford, England.

[1] A. L. Schawlow and C. H. Townes, Phys. Rev. 112, 1940 (1958).

POSSIBILITY OF PRODUCTION OF NEGATIVE TEMPERATURE IN GAS DISCHARGES

A. Javan
Bell Telephone Laboratories, Murray Hill, New Jersey
(Received June 3, 1959)

In a recent paper[1] Schawlow and Townes have discussed a possibility for obtaining maser action in the optical region. In their proposed scheme, negative temperature is obtained by optical pumping. One may expect also that under favorable conditions the excitation of atomic levels by electrons in a discharge can lead, in principle, to a state of negative temperature. However, severe restrictions exist if densities of the excited atoms as large as those needed for maser action are required. The present Letter considers briefly these limitations and certain types of systems which appear to be most favorable for practical application of this proposal. Pure gases behave quite differently than certain kinds of gas mixtures. First let us consider the former case.

For the purposes of rough estimates of various discharge conditions as described below, let us make a simplifying assumption that the main source of population of an excited state is due to collisions of the first kind between the electrons and atoms in the ground state leading directly to the excited level under consideration. It can be shown that, at least in cases discussed below, other details such as cascade processes and collision of electrons with other excited atoms do not appreciably effect our order-of-magnitude estimates.

In the following, the indices 0, 1, and 2 refer to the ground, the lower, and the upper states of the maser levels, respectively. If $1/\theta_{0i}$ is the rate of excitation of the ith excited state by electron impact with the atoms in the ground state and $1/\theta_{i0}$ is the rate for the reverse process, for a Maxwellian distribution of electrons at a temperature T_e, the relationship

$$\theta_{0i}/\theta_{i0} = \exp(E_i/kT_e)$$

will hold;[2] where E_i is the energy of the ith excited state. For θ_{i0} much shorter than the radiative lifetimes of the ith excited state, T_i, it can be shown that $N_i/N_0 = \exp(-E_i/kT_e)$, which means a Boltzmann equilibrium for population distribution of the excited state at the electron temperature T_e. For $\theta_{i0} \gg T_i$, however, one obtains

$$N_i/N_0 = (T_i/\theta_{i0})\exp(-E_i/kT_e). \quad (1)$$

The ratio T_i/θ_{i0} is a measure of departure from the Boltzmann equilibrium. Such a departure is necessary for the problem under consideration. The factor $1/\theta_{i0}$ is proportional to the electron density in the discharge. It is therefore clear that excessively large electron densities should be avoided in order to satisfy $\theta_{i0} \gg T_i$, so that

$$N_2/N_1 = (T_2/T_1)(\theta_{10}/\theta_{20})\exp[-(E_2 - E_1)/kT_e]$$

may be larger than unity, giving a negative temperature.

If the nature of the excited levels to be used for the maser action permits, it is very desirable to operate at a large gas pressure consistent with practical considerations. This is evident since for a given number of atoms in an excited state an effective temperature as determined from the ratio of this number to that of the atoms in the ground state is lower at larger pressure.

At a large pressure, however, the trapping of resonant radiation becomes an important factor. Consider a level which is optically connected to the ground state. At a pressure where the resonant photons arising from this transition are trapped, the effective radiative lifetime of this level will be increased and determined by its decay into the other available low-lying levels. This effect can best be taken to the advantage if the upper maser level is optically allowed to the ground state. In such a situation, in addition to an increased lifetime of the upper maser level at a large pressure, one expects also a more favorable ratio of θ_{10}/θ_{20}. This is evident since a level which is optically connected to the ground level, as a rule, has a large excitation cross section by electron impact with the atoms in the ground state. Furthermore, due to the nature of the electrical dipole matrix elements, only one of the maser levels may be optically connected to the ground level.

For a typical example of levels which allow operation at a large pressure, let us consider the case of Ne. The $2s_4$ and $2p_{10}$ (in Paschen notation)[3] considered as the upper and the lower maser levels, respectively, meet the required conditions. At a pressure where the ultraviolet photons arising from the transition $2s_4$ to the ground state are completely trapped, the lifetime of this state is estimated to be at least a factor of 60 larger than that of the $2p_{10}$ level. The latter level is known to have a mean life of 10^{-8} sec due to its radiative decay into some of the lower excited states. Let us consider 10 mm of Hg as a typical gas pressure. For production of $N_2 = 10^{10}/\text{cm}^3$, one obtains from Eq. (1), $T_2/\theta_{20} = 3\times10^{-5}$, assuming an electron temperature at $kT_e = 2.9$ ev. The cross section for electron excitation of the above Ne level is not known. Let us assume a reasonable value of $\sigma = 10^{-17}$ cm^2 for an average of this cross section over the electron energy distribution. From the above value of T_2/θ_{20} and $T_2 = 6\times10^{-7}$ sec, one obtains an electron density of $n_e = 5\times10^{10}/\text{cm}^3$.

The numbers obtained above are intended to represent only rough estimates and indicate that, in practice, the necessary discharge conditions are obtainable. Considerations such as departure from Maxwellian energy distribution of the electrons at the high- and low-energy limits may show appreciable effects. However, with view to the possibility of operating at somewhat of a higher electron temperature, no serious consequences are expected.

In the above scheme, the presence of a large density of the metastable Ne should be avoided to prevent the trapping of the red Ne line which may lead to an extended lifetime for the $2p_{10}$ level. Furthermore, the collision of the first kind of the electrons with the Ne metastables may give rise to an unfavorable population of the excited levels. This can be prevented by introducing a very small amount of a quenching gas such as argon to decrease the lifetimes of the longer lived excited atoms such as the metastables.

It may be of interest to compare the above system with a case which does not permit operation at large pressure. In He the $3\,^1D$ and $2\,^1P$ levels have a lifetime ratio of $T_2/T_1 = 35$. The lower level, $2\,^1P$, has a short lifetime due to its radiative decay into the ground level. An estimate of θ_{10}/θ_{20} indicates that this ratio may be as large as 1/15. Thus, a negative temperature may still be expected if appreciable excitation of these levels by electron impact with the metastable He can be prevented. On the basis of the known cross section for electron excitation of the $3\,^1D$

level and manipulations similar to those presented above, the following rough estimate of the discharge condition may be obtained: At a pressure of 5×10^{-3} mm and for $kT_e = 5$ ev, the electron density for production of $N_2 = 10^9/\text{cm}^3$ is roughly $n_e = 10^{12}$ or about 1% ionization of the total number of atoms. Although such a condition is not outside of the range of practical possibility, however, it indicates the difficulties encountered in this case. It is likely that a more favorable situation of this type may be found in a different atom with a larger electron excitation cross section, thus resulting in a reduced number for the required electron density.

An alternative scheme is the use of transfer of excitation between excited states of two different atoms in a gas mixture. Consider a long-lived state of an atom (such as a metastable state). This state can be populated appreciably at moderate electron densities. If an excited state of a second atom happens to lie very close in energy to that of the level of the first atom, a large cross section is expected to exist for an inelastic collision resulting in a transfer of excitation from the metastable state to the excited state of the other atom and vice versa. Due to the nonadiabatic nature of the process of collision, the levels of the second atom which differ in energy considerably from that of the metastable level of the first atom do not show appreciable cross sections for transfer of excitation.

If the rate at which such transfer of excitation takes place is larger than the rate of the radiative decay of the excited states, the metastable level serves to increase the contact between the temperature of the excited level of the other atoms and that of the electrons. In this case, it can be shown that $(G^*N^*/GN) = (g^*n^*/gn)f$, where the capital letters refer to one atomic species and the small letters to the other. The letters with asterisks denote the excited states, and those without asterisks, the ground states; G and g are the statistical weights of the levels involved and N and n are the populations of the levels. The factor f in this equation is given by $f = e^{\Delta E/kT}$, where T is the temperature of the gas as determined by thermal kinetic energies of the atoms and ΔE is the resonance defect and is the difference between the excitation energy of the level corresponding to n^* minus that corresponding to N^*.

This relationship does not hold if ΔE is appreciably large, resulting in reduced rate of transfer of excitation.

In order to take full advantage of the above effect, large differences in the partial pressures of the two atoms are desirable. Otherwise, due to reduction in electron temperature and various quenching mechanisms, the population of the metastable level will be decreased.

As an example, a mixture of Kr and Hg with Kr at about 10 to 50 mm of Hg pressure and Hg at about 10^{-3} mm of Hg pressure can be used for obtaining an abnormally large population of the $9\,^1P$ and $6\,^1F$ of Hg. These two levels lie very close to $5s_5$ metastable Kr. A negative temperature at the transition originating from these levels to $6\,^1D$ may then be expected. It is expected that the levels $6\,^1D$ and $6\,^1P$ may also show a negative temperature because of the cascade transition from the $9\,^1P$ and $6\,^1F$ into $6\,^1D$ level.

The $^3S_1$ metastable of He also lies in energy fairly close to the excitation energy of the upper maser level of Ne discussed above. The presence of a partial pressure of He is expected to enhance considerably the negative temperature in the levels of Ne.

The transfer of excitation of the type described above may play an appreciable role within the levels of the same atom. An important example of this is expected to occur in the levels of Ne. Let us consider the group of four levels $2s_5$, $2s_4$, $2s_3$, and $2s_2$. The level $2s_4$ is the one emphasized in the above for the upper of the two maser levels. These four levels all fall fairly close in energy. The level $2s_2$ is also allowed for an optical transition to the ground state. The transfer of excitation within these levels is expected to result in particular built up of large population in the level $2s_5$, this level having the lowest energy within this group. Thus, an even more favorable transition in Ne appears to be the $2s_5 - 2p_{10}$. This transition lies at 10343 wave number.

Details of the above proposals will be published upon their experimental verifications.

I would like to acknowledge helpful discussions with Dr. W. R. Bennett, Jr., Dr. S. J. Buchsbaum, Professor C. H. Townes, Dr. J. P. Gordon, and Dr. A. L. Schawlow.

---

[1] A. L. Schawlow and C. H. Townes, Phys. Rev. 112, 1940 (1958).

[2] See, for instance, Rudolf Ladenberg, Revs. Modern Phys. 5, 243 (1933).

[3] In the LS designations the levels $2s_4$ and $2p_{10}$ correspond to $(2p^5 4s)\,^3P_1$ and $(2p^5 3p)\,^3S_1$, respectively.

LAMB SHIFT AND ENERGY LEVEL OF A TIGHTLY BOUND ELECTRON

D. F. Mayers
University Computing Laboratory, Oxford, England

and

G. E. Brown and E. A. Sanderson
Department of Mathematical Physics, University of Birmingham, Birmingham, England
(Received June 1, 1959)

The K-absorption edge in mercury has been calculated to within terms of order α^2mc^2 (where $\alpha^2mc^2 = 2$ ry), with the object of verifying the presence of the Lamb shift, which is of order αmc^2. Here, we consider $Z\alpha$ to be of the order of unity, since Z is large.

Earlier rough calculations[1] to within order αmc^2 of all effects other than the Lamb shift gave a value of 6129 ry for the K-absorption edge and left an apparent discrepancy of only several Rydbergs with experiment to be accounted for by the Lamb shift. However, the experimental values were incorrectly quoted in this article, and the actual discrepancy was ~20 ry.

To improve on the calculation of effects of order mc^2 and αmc^2 other than the Lamb shift, a relativistic self-consistent-field calculation with exchange (Hartree-Fock calculation) was carried out by one of us (D.F.M.). Just as in the nonrelativistic case,[2] the energy of the electron system can be expressed in terms of one-electron radial integrals; complete expressions have been given by Swirles[3] and Grant.[4] To within order αmc^2, the K-absorption edge is given by $\epsilon_{1s} + \delta\epsilon_{1s}$, where ϵ_{1s} is the eigenvalue of the 1s state, and $\delta\epsilon_{1s}$ is the shift arising from the magnetic interaction between the K electrons. The eigenvalue was found to be 6152 ry, and $\delta\epsilon_{1s}$, -15 ry, giving a net value of 6137 ry. This is in good agreement with similar calculations by Cohen,[5] who obtains 6138 ry.

Inclusion of the Lamb shift completes the effects of order αmc^2. This calculation was carried out[6] without employing an expansion in $Z\alpha$, giving a result of -38 ry when combined with that of the vacuum polarization.[7] The resulting theoretical value of 6099 ry is to be compared with the experimental value[8] of 6107.7 ± 0.6 ry for the K-absorption edge, showing that inclusion of the Lamb shift markedly improves the agreement.

Corrections of order α^2mc^2 are contributed by the rearrangement energy and by the finite size of the nucleus. The former was evaluated by repeating the relativistic self-consistent-field calculations for the ionized atom, $Hg^+(1s)^{-1}$, giving a result of 4 ry.

The correction from the finite size of the nucleus was calculated using[9]

$$G_0^2\delta y|_{R_1} - G_0^2\delta y|_{R_2} = \int_{R_1}^{R_2}\left\{\frac{G_0^2}{G^2}(G^2+F^2)(\delta E-\delta V) + G_0^2(E+m-V)(\delta y)^2\right\}dr, \quad (1)$$

where F, G, and F_0, G_0 are the perturbed and unperturbed Dirac radial functions, multiplied by r, respectively, $y = F/G$, $y_0 = F_0/G_0$, and $\delta y = y - y_0$. Here, R_1 was chosen to be a radius just outside the nuclear radius, and R_2 to be an appreciable fraction of the radius of the K shell. The δy was calculated by numerical integration of the differential equation from which Eq. (1) was obtained. The correction to the energy level from a nucleus with shape represented by an inverted Fermi distribution[10] was -3.9 ry, effectively cancelling the rearrangement energy.

We believe that the discrepancy of ~8 ry comes mainly from the inadequacy of the self-consistent-field method in describing correlation in angle of the two K electrons, which tend to stay apart because of their mutual repulsion.

[1] S. Brenner and G. E. Brown, Proc. Roy. Soc. (London) A218, 422 (1953).
[2] D. R. Hartree, Calculation of Atomic Structures, (John Wiley and Sons, New York, 1955), Chap. 8.
[3] B. Swirles, Proc. Roy. Soc. (London) A152, 625 (1935).
[4] I. P. Grant (to be published).
[5] S. Cohen (to be published).
[6] G. E. Brown and D. F. Mayers, Proc. Roy. Soc. (London) A251, 105 (1959).
[7] N. K. Kroll and E. H. Wichmann, Phys. Rev. 101, 843 (1956).
[8] D. Saxon, thesis, University of Wisconsin, 1954 (unpublished).
[9] G. Breit and G E. Brown, Phys. Rev. 76, 1307 (1949).
[10] Hahn, Ravenhall, and Hofstadter, Phys. Rev. 101, 1131 (1956).

ATOMIC MOTIONS IN WATER BY SCATTERING OF COLD NEUTRONS

D. J. Hughes, H. Palevsky, W. Kley,* and E. Tunkelo†
Brookhaven National Laboratory, Upton, New York
(Received June 26, 1959)

The scattering of very slow, or "cold," neutrons is a useful technique for study of the motions of atoms in solids and liquids. In this method, as developed[1] at Brookhaven, a beam of approximately 0.005-ev neutrons, produced by beryllium filtration, is incident on a thin sample. Measurement of the changes in energy at scattering gives directly the desired information concerning the atomic motions in the sample. As the energy changes are usually large compared with the incident energy, they can be measured accurately. In the case of an incoherent scatterer, such as hydrogen, a further advantage of the cold neutron technique obtains; essentially all motions of the atoms can be measured because all momentum gains are possible. The cold-neutron method was applied to water in the present experiments because of the intrinsic interest of the atomic motions and because the inelastic scattering of neutrons in water has an important bearing on its function as a reactor moderator.

The water samples, which were extremely thin, ranging down to 0.2 mm, were formed by an aluminum sample holder containing milled portions of the correct thickness separated by supporting ribs. The neutrons scattered at 90° were passed through a slow chopper and the energies measured by time of flight to detectors five meters distant, as already described.[1] Careful background runs were made with empty sample holders and the spectrum shape of the incident neutrons was determined by scattering from a thin sheet of vanadium, which is essentially an elastic incoherent scatterer. The spectrum of scattered neutrons is shown on a time-of-flight scale in Fig. 1, corrected for instrumental effects. The results were somewhat unexpected in that they show a number of definite energy levels, rather than a continuum of energy changes that would be expected from a classical liquid. Because of the quantum nature of water thus revealed it appears that it is not a suitable material for simple application of the theory of scattering of neutrons by liquids developed by Vineyard,[2] on the basis of the more general theory of Van Hove.[3]

Further investigations are being made on these various features, particularly as a function of sample temperature, and only the most signifi-

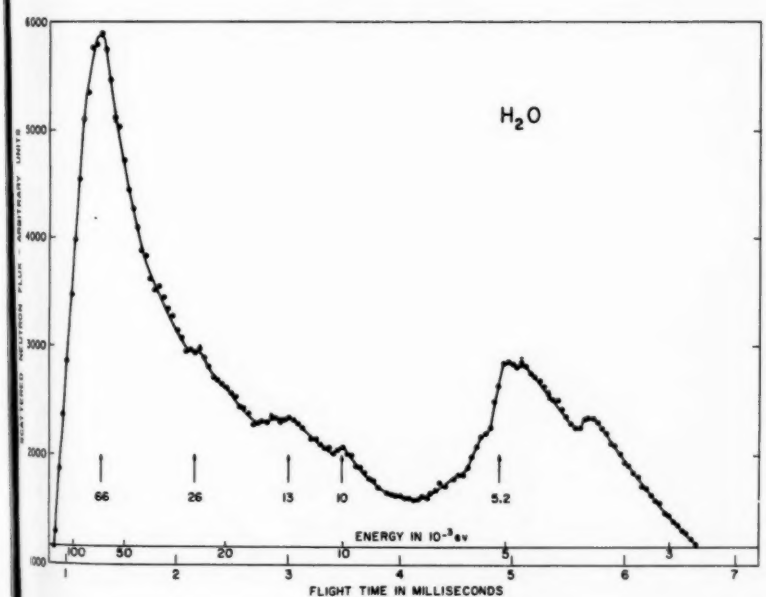

FIG. 1. Neutron flux observed at 90° from incident beam direction. Data are corrected for counter efficiency and chopper transmission. The arrow at 5.2×10^{-3} gives the position of the Bragg cutoff for the Be-filtered incident spectrum. The other arrows give the measured neutron energies corresponding to hindered motions of the liquid. The quantum energy of these states is the difference between the indicated energy and 5.2×10^{-3} ev, the incident energy.

cant will be considered here. The prominent energy gain of magnitude 0.061 ev has been found much earlier by infrared measurements[4] and interpreted as a hindered rotation, that is, a rotatory oscillation of one water molecule in the field of its neighbors. Infrared measurements are not possible at energies much lower than that of the hindered rotations, whereas the present technique extends about a hundredfold lower, to the region of microwave absorption. At energies below that of the hindered rotation there are a number of peaks, which are probably to be associated with various types of translatory motions of water molecules in the potential of their neighbors.[4]

A most surprising effect observed is the extremely small energy changes shown by the two peaks near the energy of the incident neutrons (Figs. 1 and 2), representing the transfer of energy from and to the liquid of the same amount, 0.7×10^{-3} ev. This energy is much less than that of the other energy changes found in water and there is no known transition in liquid water that could account for it. The observed energy actually corresponds closely to a line recently observed[5] in the microwave spectrum of water vapor, although it would be very surprising for this energy transition to appear in the liquid.

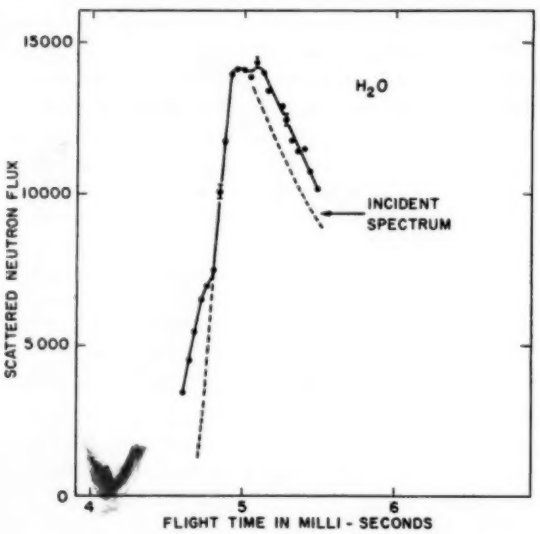

FIG. 2. The details of the scattered spectrum near the "elastic peak." The dashed curve shows the position of the incident spectrum as would be measured with a thin vanadium scatterer. The water data are seen to coincide with the incident spectrum in the region of the sharp rise, indicating little diffusive scattering. The two small peaks at energies lower and higher than the sharp edge correspond to neutron energy loss and gain of 0.7×10^{-3} ev.

The low incident energy in the present experiment should be particularly suitable for observing the small energy changes arising from diffusive motions of the atoms. Vineyard has considered the slight energy broadening of the incident spectrum and in one simple model the energy spread, $\Delta\epsilon$, is given directly by the diffusion constant

$$\Delta\epsilon \cong 2\hbar D k_0^2, \tag{1}$$

where $\hbar k_0$ represents the momentum transferred to the scattered neutron. The surprising finding of the present work is, however, that no spreading of the incident beam is observed (Fig. 2), although for the experimental conditions one would expect from Eq. (1) a spreading of 0.9×10^{-3} ev, which would be easily observed. A careful analysis of the present results shows that a diffusion spreading of 0.3×10^{-3} ev could have been detected, and hence the observed spread is certainly less than one-third of the calculated value. In similar measurements with water at 45°C, the upper limit is even lower, about one-sixth.

The present results indicate that the so-called "jump time" for diffusion, instead of being equal to the reciprocal of the Debye frequency, which is about 10^{-12} second in water, is at least six times longer. This finding indicates that the water molecule remains in its initial position for a number of vibrations before jumping to a new position. The magnitude of the jump would then have to extend over several molecules in order to obtain agreement with the known diffusion constant.

In order to clarify further the results just discussed, additional measurements are being made at higher temperatures and for vapor and ice as well as for liquid D_2O. As far as the application to moderation of neutrons in reactors is concerned, the small energy changes here presented are of little significance relative to the extremely prominent interchange of energy with the hindered rotation. The results also show that the motions in water are not represented well by a gas consisting of points of mass 18, an approximation often used in reactor calculations.

Brockhouse[6] has made similar measurements on water, with both low- and high-energy incident neutrons. His results with high-energy incident neutrons, as expected, do not reveal the details shown by the present measurements.

Both his results and ours with cold neutrons reveal the hindered rotation but there are marked differences concerning the other features. His measurements do not show the sharp peaks that we have observed, particularly those corresponding to the small energy changes. Instead of the latter, he observes a general broadening of the elastic peak, which is somewhat smaller than that expected from diffusive motions. This result is in sharp contrast to ours, which shows no evidence of broadening related to diffusive motions.

*Guest scientist from University of Freiburg, Freiburg, Germany.

†Guest scientist from Finland Institute of Technology, Helsinki, Finland.

[1]Eisenhauer, Pelah, Hughes, and Palevsky, Phys. Rev. 109, 1046 (1958).

[2]G. H. Vineyard, Phys. Rev. 110, 999 (1958).

[3]L. Van Hove, Phys. Rev. 95, 249 (1954).

[4]M. Magat, Ann. Physik 6, 108 (1936).

[5]C. H. Townes (private communication).

[6]B. N. Brockhouse, Phys. Rev. Letters 2, 287 (1959).

SCATTERING OF 50- to 140-Mev PHOTONS BY PROTONS AND DEUTERONS*

L. G. Hyman,† R. Ely,‡ D. H. Frisch,‖ and M. A. Wahlig**
Physics Department and Laboratory for Nuclear Science, Massachusetts Institute of Technology, Cambridge, Massachusetts

(Received June 18, 1959)

The Compton scattering of photons by protons has been studied in several experiments[1-4] below π-meson photothreshold, and in two experiments[5,6] above. We report here further work below meson threshold using both protons and deuterons as targets.

The techniques of identifying and measuring the energy of the bremsstrahlung x-rays from the M.I.T. synchrotron after they are scattered by thin targets are essentially as reported in Pugh et al.[1] The many changes which have been made in the synchrotron itself, giving it greater stability and intensity, have been described in recent M.I.T. progress reports.[7] The many changes in construction and performance of the photon telescope, energy-measuring liquid scintillator, and especially electronics, are being reported elsewhere.[8]

In Fig. 1 experimental and theoretical cross sections for scattering of photons by hydrogen are plotted as a function of lab energy at a c.m. angle of 90°. The cross sections are given per unit solid angle in the c.m. system for direct comparison with the Illinois points[5] and those of other groups.[2-4] Our results are given as a shaded area within which the cross section must lie in order to give, after appropriate folding, a fit to a smooth curve through our observed data. A discussion of this technique, which of necessity assumes a fairly smooth cross section, is given by Pugh et al.[1] The statistical standard deviation is represented by the height of the shaded area,

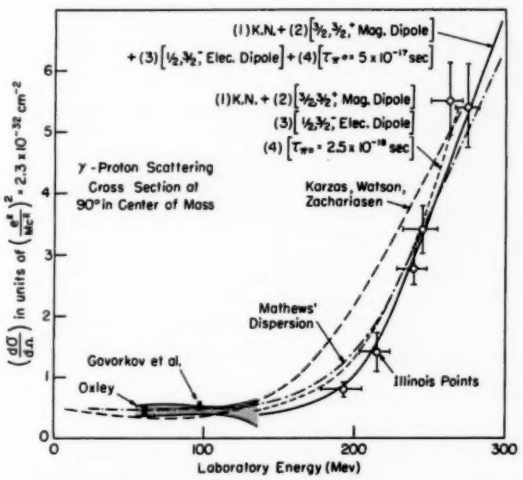

FIG. 1. Differential cross sections for scattering of 50-280 Mev photons by hydrogen at 90° c.m.

but statistical errors are thereby exaggerated somewhat, since the data were taken in channels of approximately 10 Mev, but the cross section at most energies is averaged by the counter response over an energy band of about 20 Mev. On the other hand, a possible 10% error in absolute normalization is not displayed. We see in Fig. 1 that these new data, and the results of the other experiments at this angle, are all in good agreement below meson threshold and fit in smoothly with the Illinois data.

The dashed lines in Fig. 1 are the predictions of previous calculations. As has been pointed out before,[9] the Mathews dispersion theory curve[10] is clearly too high in the 160-200 Mev region.

The meson-theoretic prediction, Karzas et al.,[11] falls somewhat too low in the region below meson threshold and rises far above the data in the 200-Mev region.

We calculated the solid curve using for each polarization the coherent addition of four amplitudes:

(1) The Klein-Nishina amplitude for scattering by a point Dirac particle. Note that this is not the Powell[12] (Dirac particle with added Pauli moment) amplitude[13]; that is, in this energy region we will describe the anomalous electromagnetic properties of the proton in terms of its excited states.

(2) The induced magnetic dipole resonance amplitude for scattering by the $T=3/2$, $J=3/2^+$ first excited state of the proton, following Austern,[14] Feld,[15] and Yamaguchi.[16] Phase shifts taken from the Chew-Low-Chiu-Lomon[17] analysis of the π-nucleon interactions were used in the single-level approximation.[11]

(3) The induced electric dipole resonance amplitude for scattering by the $T=1/2$, $J=3/2^-$ second excited state of the proton.[18-21] This crude but honest single-level calculation was patterned after Feld's "atomic model" calculation of (2) above.

(4) The amplitude shown by Low[22] to result from the special coupling of a pair of photons to a proton through the decay of a virtual π^0 meson, which thus is a function of the (unknown) π^0 mean life τ_{π^0}.

The sum of amplitudes (1), (2), and (4) gives approximately the same result (not shown) as the Mathews dispersion theory, which was evaluated prior to knowledge of the 1/2, 3/2$^-$ resonance, provided that $\tau_{\pi^0} \geq 2\times10^{-18}$ sec, but does not give a very good fit to the data. This discrepancy is removed by addition of amplitude (3), resulting in the excellent fit given by the solid line in Fig.1.

The γ-d cross section, completely in the laboratory system, is given along with the γ-p cross section in Fig. 2(a). Note that our detector has insufficient energy resolution ot make possible the separation of coherent elastic scattering by the whole deuteron from incoherent quasi-elastic scattering by the constituent proton or neutron. At 90° lab and 100 Mev one expects[23] roughly half elastic and half inelastic. The dashed curve is constructed from Mathews' nucleon amplitudes[10] in the impulse approximation,[24] using a Hulthén wave function matched to electron scattering by deuterium.[25] Judging by Mathews' curve in Fig.1, we expect the calculation to give an upper limit to the deuteron cross section. But the observed deuteron cross section seems to be about 1.6±0.3 times the hydrogen cross section over the whole energy range. Since the deuterium run was bracketed by two halves of the hydrogen run, under identical conditions, we find no way to explain this high ratio.

The cross sections for H and D at 50° are given in Fig. 2(b). The sharp rise at energies below

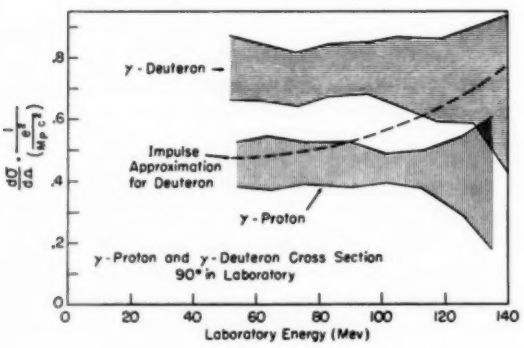

(a)

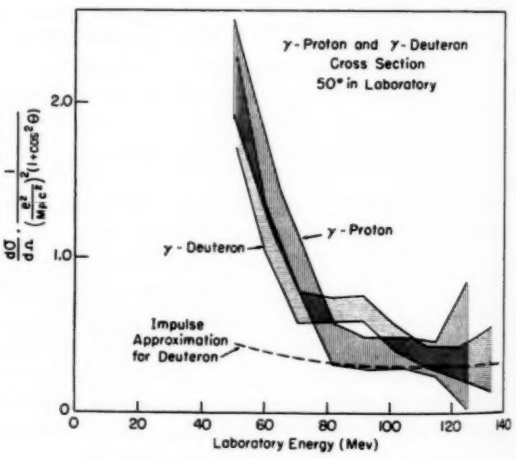

(b)

FIG. 2. (a) Differential cross sections for scattering of 50-140 Mev photons by hydrogen and deuterium at 90° lab. (b) Differential cross sections for scattering of 50-140 Mev photons by hydrogen and deuterium at 50° lab.

80 Mev is very probably not Compton scattering; the most probable origin of this low-energy background will be discussed below. The cross sections above 80 Mev are not very accurate, and we can say only that (1) the hydrogen data above 80 Mev are fitted well by Mathews' dispersion curve and (2) around 80 Mev the deuterium cross section is appreciably greater than the hydrogen cross section but seems to drop off as the energy rises near meson threshold. Because of the complexity of the deuteron problem, especially in this region of momentum transfers, and with the necessity of including all four types of elementary amplitudes listed above, no attempt has been made to interpret the 50° deuterium data.

A brief study was made of the 50° low-energy background, which had been observed previously[1] and ascribed to inner bremsstrahlung accompanying pair production (radiative pair production). But as estimated by Feynman and Gomez,[26] the intensity of inner bremsstrahlung is not sufficient to account for most of this large background. We therefore measured, using a carbon target, the number of electrons coming to the detector from the target, and found that there were enough to produce the observed spectrum of gamma rays at low energies by bremsstrahlung in the rather thick beryllium shield[27] in front of the counter telescope. The dependence of this background on target thickness and machine energy is in agreement with what would be expected from the number of wide-angle pair electrons[25] produced in the target plus the Mott scattering of small-angle electrons produced both in the target and upstream from it.

We conclude: (1) the observed scattering of photons by protons at 90° c.m. over the energy range 0-300 Mev is described well by a model of the proton as a Dirac particle plus strong pion interactions giving the well-known 3/2, $3/2^+$ and 1/2, $3/2^-$ resonances, provided the half-life of the π^0-meson is greater than 10^{-18} second. (2) The scattering of photons by deuterons below meson threshold is more than expected.

We thank D. Luckey, L. Osborne, and the M.I.T. Synchrotron staff for generous help with the experiment; B. Feld, M. Friedman, F. Low, C. Nielsen, F. Villars, and V. Weisskopf for stimulating discussions; and the U.S. Atomic Energy Commission, the Office of Naval Research, the Office of Scientific Research, the National Science Foundation, the General Electric Company, and the Sloan Foundation for their generous support.

*This work is supported in part by funds provided by the U.S. Atomic Energy Commission, the Office of Naval Research, and the Air Force Office of Scientific Research.

†Present address: Harvard University, Cambridge, Massachusetts.

‡General Electric Fellow.

‖Sloan Fellow.

**National Science Foundation Predoctoral Fellow.

[1]Pugh, Gomez, Frisch, and Janes, Phys. Rev. 105, 982 (1957).

[2]Govorkov, Goldanski, Karpuhkin, Katsenko, and Pavlovskaya, Doklady Akad. Nauk. SSSR 111, 988 (1956) [translation: Soviet Phys. Doklady 1, 735 (1956)].

[3]C. L. Oxley, Phys. Rev. 110, 733 (1958).

[4]Alvarez, Crawford, and Stevenson, Phys. Rev. 112, 1267 (1958).

[5]Auerbach, Bernardini, Filosofo, Hanson, Odian, and Yamagoda, Proceedings of the CERN Symposium on High-Energy Accelerators and Pion Physics, Geneva, 1956 (CERN Scientific Information Service, Geneva, 1956), p. 291.

[6]Littauer, DeWire, and Feldman, Bull. Am. Phys. Soc. 4, 253 (1959).

[7]D. Luckey, L. S. Osborne, et al., Massachusetts Institute of Technology Laboratory for Nuclear Science Progress Report, 1958 (unpublished).

[8]L. G. Hyman, Massachusetts Institute of Technology Ph.D. thesis, 1959 (unpublished).

[9]G. Bernardini, 1958 Annual International Conference on High-Energy Physics at CERN, edited by B. Ferretti (CERN Scientific Information Service, Geneva, 1958).

[10]J. Mathews, California Institute of Technology, Ph.D. thesis, 1957 (unpublished).

[11]Karzas, Watson, and Zachariasen, Phys. Rev. 110, 253 (1958).

[12]J. L. Powell, Phys. Rev. 75, 32 (1949).

[13]R. Gomez and D. Walecka, Phys. Rev. 104, 1479 (1956).

[14]N. Austern, Phys. Rev. 100, 1522 (1955).

[15]B. T. Feld, Ann. Phys. 4, 189 (1958).

[16]See mention in T. Yamagoda, University of Illinois Ph.D. thesis, 1956 (unpublished).

[17]H. Y. Chiu and E. L. Lomon, Ann. Phys. 6, 50 (1959).

[18]R. R. Wilson, Phys. Rev. 110, 1212 (1958).

[19]F. P. Dixon and R. L. Walker, Phys. Rev. Letters 1, 142 (1958).

[20]P. C. Stein, Phys. Rev. Letters 2, 11 (1959).

[21]R. Peierls, Phys. Rev. Letters 1, 174 (1958).

[22]F. E. Low (private communication). This amplitude was taken with the sign indicated by the perturbation theory treatment of π^0-decay. If the opposite sign were taken, the best fit would be for $\tau=\infty$, and the data would set a lower limit of about $\tau \geq 5\times 10^{-17}$ sec.

[23]R. H. Capps, Phys. Rev. 106, 1031 (1957).

[24]G. Chew and H. Lewis, Phys. Rev. 84, 779 (1951).

[25]J. McIntyre, Phys. Rev. 103, 1464 (1956).

[26]R. P. Feynman and R. Gomez (private communication).

[21]This beryllium shield was several times thicker, in radiation lengths, than similar shields used in other experiments.

[22]R. C. Miller, Phys. Rev. 95, 796 (1954).

A FORMAL OPTICAL MODEL

J. S. Bell and E. J. Squires
Atomic Energy Research Establishment, Harwell, England
(Received June 15, 1959)

A construction is given of an equivalent one-body potential for the elastic scattering of a particle incident on a complex target. We consider explicitly the case that incident and target particles are identical nonrelativistic fermions and allow fully for antisymmetry. The method is inspired by that of Frantz and Mills[1] and removes some defects therefrom; it also removes the basis for their proposed change in phenomenological optical model analysis. Center-of-mass motion is still ignored.

Denoting by $|\bar{\alpha}\rangle$ the scattering state and by $|\bar{0}\rangle$ the target ground state, we define the model wave function as

$$\phi(\vec{r},t)=\langle\bar{0}|\bar{\psi}(\vec{r},t)|\bar{\alpha}\rangle, \tag{1}$$

where $\bar{\psi}$ is the Heisenberg field operator of second quantization. For $|\bar{\alpha}\rangle$ we take the state

$$|\bar{\alpha}\rangle=\int_{-\infty}^{t}dt'e^{-iEt'}\bar{\psi}^{\dagger}(\vec{r}',t')|\bar{0}\rangle, \tag{2}$$

which corresponds to a source of particles of energy E at the point $\vec{r}'$; if r' is sufficiently large only a plane wave actually reaches the target. In writing, with $x\equiv(\vec{r},t)$,

$$\phi(x)=\int_{-\infty}^{+\infty}dt'e^{-iEt'}G(x,x'), \tag{3}$$

$$G=\langle\bar{0}|T(\bar{\psi}(x),\bar{\psi}^{\dagger}(x'))|\bar{0}\rangle, \tag{4}$$

we make no error by taking the time-ordered rather than the retarded product, for the surplus contribution depends on the possibility of absorbing a particle at $\vec{r}'$ from the state $|\bar{0}\rangle$ and so vanishes for large r'.

We construct G by a perturbation theory where in zero order the real forces are replaced by a fictitious one-body potential, in general nonlocal,

$$\int d\vec{r}d\vec{r}'\,\bar{\psi}^{\dagger}(\vec{r},0)U(\vec{r},\vec{r}')\bar{\psi}(\vec{r}',0).$$

An S matrix is defined by

$$\frac{\partial}{\partial t}S(t,t')=-iH'(t)S(t,t'),$$

$$S(t',t')=1,\quad H'(t)=e^{iH_0t}H'e^{-iH_0t},$$

where H_0 is the zero-order Hamiltonian and the total Hamiltonian is H_0+H'. In terms of interaction representation operators ψ, the Heisenberg operator $\bar{\psi}$ can be written

$$\bar{\psi}(x)=S^{-1}(t,0)\psi(x)S(t,0),$$

and we have the usual expression

$$G=\frac{\langle 0|S(\infty,t)\psi(x)S(t,t')\psi^{\dagger}(x')S(t',-\infty)|0\rangle}{\langle 0|S(\infty,-\infty)|0\rangle},$$

for $t>t'$, and similarly for $t<t'$, where $|0\rangle$ is the zero-order target ground state—assumed nondegenerate. Expanding above and below in powers of H', we have

$$G=\sum_{n=0}^{\infty}\frac{1}{n!}\int dt_1\cdots dt_n\langle 0|T\{H'(t_1)\cdots H'(t_n)\psi(x)\psi^{\dagger}(x')\}|0\rangle\Big/\sum_{n=0}^{\infty}\frac{1}{n!}\int dt_1\cdots dt_n\langle 0|T\{H'(t_1)\cdots H'(t_n)\}|0\rangle. \tag{5}$$

We make a diagrammatic analysis of this following Hubbard,[2] using Wick's theorem and regarding $|0\rangle$ as "vacuum." The denominator has the effect simply of cancelling all diagrams in the numerator not linked to the terminal operators $\psi(x)$ and $\psi^{\dagger}(x')$; G is therefore the sum of linked diagrams only from the numerator. We call "improper" a linked diagram which falls into two disconnected parts on the removal of some particle (as distinct from interaction) line. Reasoning familiar

in field theory leads to the integral equation

$$G(x,x') = G_0(x,x') - iG_0(x,x'')W(x'',x''')G(x''',x'), \tag{6}$$

where repeated arguments are integrated over, G_0 is the zero-order value, and $-iW$ is the sum of all proper linked diagrams—omitting factors for the terminal lines. Then from (3) with $t=0$,

$$\phi(\vec{r}) = \phi_0(\vec{r}) - iG_0(E,\vec{r},\vec{r}')W(E,\vec{r}',\vec{r}'')\phi(\vec{r}''), \tag{7}$$

where

$$W(E,\vec{r},\vec{r}') = \int d(t-t')\, e^{iE(t-t')} W(x,x'), \tag{8}$$

and likewise for G_0.

Now if u_n are a complete set of wave functions for the potential U, with eigenvalues E_0,

$$-iG_0 = \sum^{\text{unocc.}} \frac{u_n(\vec{r})u_n^*(\vec{r}')}{E-E_n+i\epsilon} + \sum^{\text{occ.}} \frac{u_n(\vec{r})u_n^*(\vec{r}')}{E-E_n-i\epsilon}.$$

Since all the occupied states are of negative energy, for positive E the sign of the infinitesimal $i\epsilon$ is unimportant in the last term. Thus

$$\phi(\vec{r}) = \phi_0(\vec{r}) + \sum_n \frac{u_n(\vec{r})u_n^*(\vec{r}')}{E-E_n+i\epsilon} W(E,\vec{r}',\vec{r}'')\phi(\vec{r}''). \tag{9}$$

This is just the integral equation for scattering by an added potential W, and therefore

$$V(E,\vec{r},\vec{r}') = U(\vec{r},\vec{r}') + W(E,\vec{r},\vec{r}') \tag{10}$$

is the total optical potential. The scattering amplitude averaged over an interval of energy can be obtained from $V(E+i\epsilon,\vec{r},\vec{r}')$ with ϵ finite. This and other details will be discussed elsewhere.

In conclusion we compare this account with that of Frantz and Mills. They define an optical model wave function by projecting on to the zero-order rather than the real target ground state:

$$\phi'(\vec{r},t) = \langle 0|\bar{\psi}(\vec{r},0)|\bar{\alpha}\rangle. \tag{11}$$

In the diagrammatic analysis it is then natural to use time-ordered rather than Feynman diagrams. As a result, for example, the two diagrams of Fig. 1 are regarded as distinct and the second as "proper." The proper parts of diagrams are now connected by forward lines

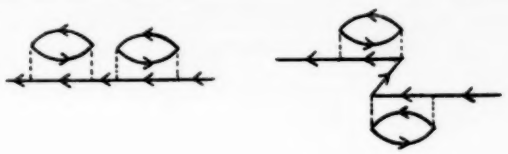

FIG. 1. Time-ordered diagrams.

only (particles) and not backward lines (holes). In the equation replacing (9) the n summation then runs over unoccupied states only, and the optical potential is therefore of the form

$$U + PW',$$

where P is a projection operator on to unoccupied states. Even in the trivial case that the perturbation is only a change ΔU in the one-body potential, the "optical" potential based on U would have this form. In contrast, our development gives in this case the natural result $V = U + \Delta U$.

A more serious objection to the use of (11) as an optical model wave function is that it does not have an acceptable asymptotic form when inelastic scattering is possible. If $|\bar{n}\rangle$ denotes a state of excitation Δ_n of the target, then asymptotically

$$\langle \bar{n}|\bar{\psi}(\vec{r},0)|\bar{\alpha}\rangle \sim f_n r^{-1} e^{iK_n r},$$

with

$$K_n^2 = K_0^2 - 2M\Delta_n.$$

If

$$\langle 0| = \sum \xi_n \langle \bar{n}|,$$

then ϕ' has an outgoing part

$$\sum \xi_n f_n r^{-1} e^{iK_n r},$$

which is a superposition of inelastic as well as elastically scattered waves.

---

[1] L. M. Frantz and R. L. Mills (to be published); Frantz, Mills, Newton, and Sessler, Phys. Rev. Letters 1, 340 (1958).

[2] J. Hubbard, Proc. Roy. Soc. (London) A240, 539 (1957).

PROTON-NEUTRON INTERACTION AND THE (p,n) REACTION IN MIRROR NUCLEI*

S. D. Bloom
Lawrence Radiation Laboratory, University of California, Livermore, California

N. K. Glendenning
Lawrence Radiation Laboratory, University of California, Berkeley, California

and

S. A. Moszkowski
Department of Physics, University of California, Los Angeles, California
(Received June 10, 1959)

Direct-interaction reactions have been treated by a number of authors[1] from the point of view of obtaining information concerning spins and parities of excited states of nuclei. The purpose of this note is to point out a new use of this type of reaction—a study of the direct interaction itself.

It should be emphasized that the direct interaction referred to is the effective neutron-proton potential within the nucleus. Recent theoretical studies indicate that this effective interaction is essentially the long-range part (distances $\gtrsim 10^{-13}$ cm) of the actual two-nucleon interaction.[2] The (p,n) reactions on mirror nuclei are a particularly promising source of information on this effective interaction, as will be developed below.

Consider as an example, the mirror nucleus reaction

$$C^{13}(p,n)N^{13} \tag{1}$$

going to the ground state.[3] [It can be shown that the (p,n) reaction is equivalent in the view adopted here for the two cases, doubly closed shells plus one neutron or minus one proton. For example, the ground-state reactions $C^{13}(p,n)N^{13}$ and $N^{15}(p,n)O^{15}$ should be twin reactions.[4]] In the j-j coupling shell model, the last neutron in C^{13} lies beyond doubly closed neutron and proton subshells.[5] The (p,n) reaction is regarded as involving only the neutron beyond the C^{12} core. The interaction between this extra-core neutron and the incident proton is written

$$\mathcal{V} = V_a + V_b P^{\tau}, \tag{2}$$

where V_a and V_b are in general spin-dependent central potentials and P^{τ} is the isotopic spin exchange operator. The antisymmetric wave functions for initial and final states appropriate to the reaction (1) are

$$|i\rangle = \frac{1}{\sqrt{2}}\{|1,2\rangle\pi(2)\nu(1) - |2,1\rangle\pi(1)\nu(2)\}, \tag{3}$$

$$|f\rangle = \frac{1}{\sqrt{2}}\{|1,2\rangle\pi(1)\nu(2) - |2,1\rangle\pi(2)\nu(1)\}, \tag{3'}$$

where $|1,2\rangle$ denotes a state with nucleon 1 bound by the C^{12} core, and nucleon 2 free, and π and ν are isotopic spin functions corresponding to proton and neutron states, respectively.

The matrix element of $\mathcal{V}$ taken between the initial and final states (3) and (3′) is

$$\langle f|\mathcal{V}|i\rangle = \langle 1,2|V_b|1,2\rangle - \langle 1,2|V_a|2,1\rangle. \tag{4}$$

Thus the matrix element of $\mathcal{V}$ separates into two parts, one of which is a "direct" matrix element, $\langle V_b\rangle$, and the other an "exchange" matrix element, $\langle V_a\rangle$. The "direct" matrix element refers to the charge exchange process in which the charge on the incident proton is transferred to the bound neutron. The "exchange" matrix element refers to the knock-out process in which the incident proton is captured, knocking out the extra-core neutron.

We may ignore the exchange integral in (4) compared to the direct integral because of the poor overlap of the bound and free states wave functions on the one hand and on the other hand, the good overlap of the extra-core neutron wave function in C^{13} with the extra-core proton wave function in N^{13}. It is emphasized that in mirror nuclei, this overlap argument should be particularly valid, because, aside from Coulomb distortion, the bound-state wave functions that enter the matrix elements are identical. Another way of looking at this is to realize that the direct integral refers to forward scattering, while the exchange integral refers to back scattering. We know that if the scattering of two particles interacting through a potential is calculated, say in Born approximation, the forward scattering (small momentum transfer) is much larger than the back scattering (large momentum transfer).

In the above approximation therefore, the (p,n) reaction connecting ground states of mirror

nuclei singles out the isotopic spin exchange part, V_b, of the neutron-proton interaction inside nuclei. Thus a comparison of the experimental cross section for this reaction with a detailed theoretical calculation of the cross section ought to provide the potential V_b of (2). It is important to note that no one has yet succeeded in calculating the correct absolute magnitude of the cross section for a direct interaction process. Levinson and Banerjee[6] have given the most complete treatment in their study of proton inelastic scattering from C^{12}. They found it necessary to use a direct interaction with a strength of more than twice the free nucleon-nucleon potential. These authors suggested that the increased effective interaction may arise from a polarization of the nucleons in the target nucleus. This effect would of course be absent in the interaction (1), if it is correct to think of the target nucleus as an inert core plus one neutron in a well-defined state. Moreover the (p,n) reaction involves unambiguously a nucleon-nucleon interaction, whereas inelastic scattering by direct interaction may proceed by particle excitation in the target, or by excitation of a collective state, and these two modes are not necessarily easily distinguished.[7]

Thus the (p,n) reactions connecting the ground states of mirror nuclei are particularly suited to a rather direct measurement of the effective proton-neutron interaction in nuclei, or more specifically the charge exchange part of the interaction.

---

*This work was supported in part by the U. S. Atomic Energy Commission.

[1]Many references to the earlier work can be found in J. S. Blair and E. M. Henley, Phys. Rev. 112, 2029 (1958). See also N. K. Glendenning, Phys. Rev. (to be published).

[2]S. A. Moszkowski, Office of Ordnance Research Technical Report No. 2, University of California at Los Angeles, April, 1959 (unpublished).

[3]Recent measurements of the angular distribution of neutrons from this reaction are reported in S. D. Bloom and R. D. Albert, Bull. Am. Phys. Soc. 4, 321 (1959); see also Albert, Bloom, and Glendenning (to be published).

[4]This point as well as some others briefly referred to throughout this Letter are developed in detail in a University of California Radiation Laboratory Report now in preparation.

[5]Evidence strongly supporting the extreme j-j coupling shell model for this case is given in M. K. Banerjee and C. A. Levinson, Ann. Phys. 2, 499 (1957).

[6]C. A. Levinson and M. K. Banerjee, Ann. Phys. 2, 471 (1957); 2, 499 (1957); 3, 67 (1958).

[7]H. Ui, Progr. Theoret. Phys. (Kyoto) 18, 163 (1957); N. K. Glendenning, Ph.D. thesis, Indiana University, 1958 (unpublished).

ELECTROMAGNETIC CORRECTIONS TO THE B^{12}-N^{12} β-SPECTRUM RATIO*

Murray Gell-Mann and S. M. Berman
Norman Bridge Laboratory of Physics, California Institute of Technology, Pasadena, California
(Received June 19, 1959)

It has recently been suggested[1] that a precise comparison of the β spectra of B^{12} and N^{12} transitions to the ground state of C^{12} would provide a test of the nature of the vector interaction in β decay. Let the spectrum of each transition, divided by the corresponding Fermi spectrum, be called $S(E)$, where E is the total energy of the β ray. Then define

$$R(E) \equiv S(E, B^{12})/S(E, N^{12}). \qquad (1)$$

In reference 1 it was shown that the conserved vector current theory of β decay[2] predicts the result[3]

$$R(E) \approx \text{const}(1 + AE), \qquad (2)$$

where A is determined by the width of the 15.11-Mev level in C^{12} for γ transitions to the ground state and comes out

$$A = 1.33\% \pm 0.15\% \text{ per Mev}, \qquad (3)$$

using the measurements of Hayward and Fuller,[4] subsequently confirmed by Garwin.[5]

According to the more usual theory of β decay, in which the pion is not assigned any intrinsic β-decay "charge," we may expect a formula similar to (2), but with a much smaller value of A; the reduction factor in A should be roughly the factor by which $\mu_p - \mu_n$ is reduced if the pion current contributions to this quantity are omitted. (Here μ_p and μ_n are the proton and neutron magnetic moments.) A reasonable guess is that $\mu_p - \mu_n$ would become about one Bohr magneton

rather than almost five if the pion contributions were omitted and thus in the old theory A should be something like one-fifth of the value given in (3). The B^{12}-N^{12} experiment, if carefully performed over a range of several Mev, should thus be able to distinguish the two theories.

It has been pointed out, however, by Morita[6] and Schwarzschild[7] that the spectrum ratio $R(E)$ is altered somewhat by electromagnetic effects that were ignored in reference 1. It is our purpose here to supply a new theoretical estimate of the correction factor that should be applied to Eq. (2) to take account of these effects. With respect to the processes considered by Morita, our numerical results are in agreement with his, although our method is somewhat different.

Let us state the answer first. Instead of Eq. (2), we should use

$$R(E)/f(E) = \text{const}[1 + (A + \delta A)E], \qquad (4)$$

where

$$f(E) = 1 + \frac{\alpha}{2\pi}\left\{4(z-1)\ln[(k_0-E)/(k_0'-E)] + (z-\frac{4}{3})\frac{(k_0-k_0')}{E} + z\frac{k_0^2-k_0'^2}{6E^2}\right\}, \qquad (5)$$

with α signifying the fine structure constant, k_0 the end-point total energy for B^{12}, k_0' the end-point total energy in N^{12}, and with

$$z = \frac{1}{2}\frac{E}{(E^2-m^2)^{1/2}}\ln\left[\frac{E+(E^2-m^2)^{1/2}}{E-(E^2-m^2)^{1/2}}\right] \approx \ln(2E/m) \quad \text{for } E \gg m. \qquad (6)$$

The calculated value of δA is -0.25% per Mev, to which we would like, for the sake of safety, to attach a theoretical "error" of 0.15% per Mev. This error, and, indeed, the electromagnetic correction itself, is considerably smaller than the effect being sought, and therefore the existence of the correction does not appreciably weaken the B^{12}-N^{12} experiment as a test of the conserved current theory.

In deriving this correction, we have considered the following effects, many of which are negligible:

(a) The effect of the B^{12}-N^{12} mass difference on the spectra. Insofar as the spectra are allowed, this is taken care of by factoring out the Fermi spectra as in Eq. (1). However, there are small forbidden corrections to the spectra caused by retardation effects in the axial vector coupling. These cancel between B^{12} and N^{12} except for those terms that involve the end-point energy, which is different for the two nuclei. The resulting correction is a contribution to δA of the form

$$\delta A^{(1)} = (k_0 - k_0')\{\textstyle\int\vec{\sigma}\}^{-1}\{\frac{2}{3}\int\vec{\sigma}r^2 - \frac{1}{3}\int\vec{\sigma}\cdot\vec{r}\,\vec{r}\}. \qquad (7)$$

(b) The effect of the B^{12}-N^{12} mass difference on the inner bremsstrahlung. The probability of inner bremsstrahlung for a given electron energy depends on the end-point energy. The ratio of the correction factors in B^{12} and N^{12} is finite without an infrared cutoff and is given[8] by $f(E)$ in Eqs. (4) and (5).

(c) The difference between B^{12} and N^{12} wave functions caused by electromagnetic violations of charge independence. This alters ft values but changes the spectra only through very small changes in the already small retardation terms.

(d) The effect of virtual transverse photons exchanged between β ray and nucleus. This is of order nucleon v/c compared to the Coulomb interaction between β ray and nucleus, which we go on to consider.

(e) The effect of the Coulomb interaction between β ray and nucleus on the retardation corrections to the axial vector matrix element $\int\vec{\sigma}$. This is often considered as the sum of three terms—the "finite de Broglie wavelength effect," the effect of finite nuclear size, and the Coulomb corrections to forbidden matrix elements. We treat them all together.

Since Z is small, we can treat the Coulomb field in first order perturbation theory. Between the β decay and the Coulomb interaction the nucleus is in a virtual state which may be excited. It is difficult to evaluate the sum over all the excited states and we therefore look at two opposite approximations:

I. The excitation energies of the important nuclear levels are neglected by comparison with $\hbar c/R$, where R is the nuclear radius. In other words, the nuclear motion is assumed slow compared to the velocity of light with which the β ray is traveling. Under these conditions the sum over nuclear levels can be done by closure. In physical terms, the electron sees the instantaneous positions of the various protons that are sources of the Coulomb field. This approximation should be practically valid. As a check, however, we also consider the opposite case.

II. The energies of all excited states are taken to be so large (in energy denominators) that only the ground states survive in the sum. Physically this corresponds to the electron's seeing the nucleus as a smeared-out charge distribution.

What is important for the B^{12}-N^{12} ratio is the charge distribution in C^{12} and the average of the B^{12} and N^{12} charge distributions. The latter is just the charge distribution of the excited state of C^{12} at 15.11 Mev. For simplicity we assume that to be the same as the charge distribution of the ground state.

In each case we calculate the terms of order $Z\alpha RE$ in the spectrum ratio, dropping higher orders in RE. The result in case I is a contribution to δA equal to

$$\delta A_{\mathrm{I}}^{(2)} = -4\alpha\{\int\vec{\sigma}\}^{-1}\sum_i\{\tfrac{2}{3}\int\vec{\sigma}|\vec{r}-\vec{r}_i| + \tfrac{1}{3}\int\vec{\sigma}\cdot\vec{r}(\vec{r}-\vec{r}_i)|\vec{r}-\vec{r}_i|^{-1} - \tfrac{1}{3}\int\vec{\sigma}\cdot\vec{r}(\vec{r}-\vec{r}_i)|\vec{r}-\vec{r}_i|^{-1}\}, \quad (8)$$

where the sum is extended over all protons except the decaying nucleon. In case II the result is

$$\delta A_{\mathrm{II}}^{(2)} = -4\alpha\{\int\vec{\sigma}\}^{-1}\int\rho(\vec{r}')d^3r'\{\tfrac{2}{3}\int\vec{\sigma}|\vec{r}-\vec{r}'| + \tfrac{1}{3}\int\vec{\sigma}\cdot\vec{r}(\vec{r}-\vec{r}')|\vec{r}-\vec{r}'|^{-1} - \tfrac{1}{3}\int\vec{\sigma}\cdot\vec{r}(\vec{r}-\vec{r}')|\vec{r}-\vec{r}'|^{-1}\}, \quad (9)$$

where ρ is the charge density in C^{12} in units of e.

(f) The Coulomb effect on weak magnetism itself. Since the weak magnetic effect on the spectra comes from V-A interference, it is of opposite sign in B^{12} and N^{12}. The first order Coulomb correction to it thus has the same sign in B^{12} and N^{12} and practically cancels.

(g) The Coulomb effect on the relativistic axial vector matrix element $\int\gamma_5$. Like the uncorrected $\int\gamma_5$, this has a negligible effect on the spectrum.

We have estimated $\delta A^{(1)}$, $\delta A_{\mathrm{I}}^{(2)}$, and $\delta A_{\mathrm{II}}^{(2)}$ using the shell model with harmonic oscillator wave functions adjusted in radius to give the charge distribution of Hofstadter.[9] The results are that $\delta A^{(1)} = -0.036\,\%$ per Mev, $\delta A_{\mathrm{I}}^{(2)} = -0.21\,\%$ per Mev, and $\delta A_{\mathrm{II}}^{(2)} = -0.23\,\%$ per Mev. Since case II is so close to case I and since case I is much closer to the truth, we take $\delta A = \delta A^{(1)} + \delta A_{\mathrm{I}}^{(2)} = -0.25\,\%$ per Mev.

The largest error in our result probably comes from the use of the shell model. We can estimate how bad the shell model is by using it to calculate the allowed matrix element $\int\vec{\sigma}$ for the β decay of B^{12}. The experimental matrix element is smaller by a factor of 0.4 (in absolute value—presumably the sign is right). The ratios in Eqs. (7)-(9) are probably calculated slightly better than the absolute value and we have therefore assigned an error of about 0.15 % per Mev to δA.

---

*This research has been supported by the U. S. Atomic Energy Commission and by a grant from the Alfred P. Sloan Foundation.

[1] Murray Gell-Mann, Phys. Rev. 111, 362 (1958).

[2] S. S. Gershtein and J. B. Zeldovich, Zhur. Eksptl. i Teoret. Fiz. 29, 698 (1955) [translation: Soviet Phys. JETP 2, 576 (1957)]; R. P. Feynman and M. Gell-Mann, Phys. Rev. 109, 193 (1958).

[3] Everywhere except in Eq. (6) we neglect the mass of the electron.

[4] E Hayward and E. G. Fuller, Phys. Rev. 106, 991 (1957).

[5] T. T. Lauritsen (private communication).

[6] M. Morita, Phys. Rev. 113, 1584 (1959).

[7] A. Schwarzschild, Bull. Am. Phys. Soc. 4, 79 (1959).

[8] S. M. Berman, thesis, California Institute of Technology, 1958 (unpublished); A. Sirlin and T. Kinoshita, Phys. Rev. 113, 1652 (1959).

[9] R. Hofstadter, Revs. Modern Phys. 28, 214 (1956).

PREDICTION OF DEUTERON POLARIZATION FROM d-α SCATTERING

R. J. N. Phillips
Atomic Energy Research Establishment, Harwell, England
(Received June 12, 1959)

There is current interest in possible means of producing and analyzing deuteron polarization. d-α scattering on the 1.07-Mev resonance[1-3] and the $T(d,n)He^4$ reaction[4] have been studied. The present note shows that d-α scattering can be a useful producer (and analyzer) of deuteron polarization at energies between resonances, where the weak energy dependence may be an advantage.

We have used the phase shifts of Galonsky and McEllistrem,[5] deduced from differential cross sections with the help of dispersion theory, to calculate polarization parameters in the interval between the resonances at 1.07 and 4.6 Mev (deuteron lab energy).

In the region of 2 Mev there is considerable vector polarization, increasing smoothly with

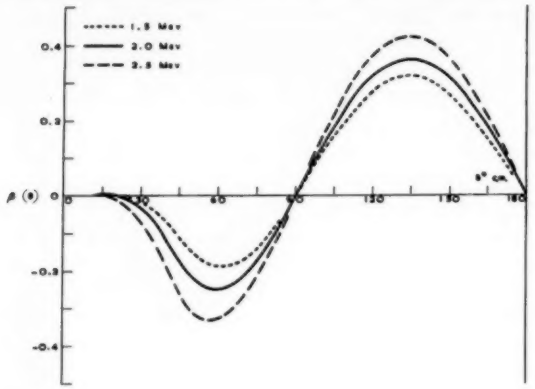

FIG. 1. d-α vector polarization near 2 Mev.

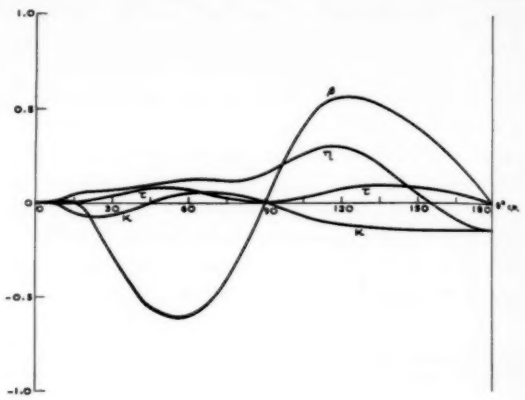

FIG. 2. d-α polarization at 3.5 Mev.

energy (Fig. 1); the tensor polarization parameters (see below) are everywhere less than 3% and are not shown. These effects come mainly from the "tail" of the $^3D_3$ resonance (1.07 Mev) interfering with potential and Coulomb scattering.

At higher energies, however, $^3D_2$ and $^3D_1$ scattering (resonances at 4.6 and ~5.9 Mev) become more important. At 3.5 Mev the vector polarization has approximately doubled, while tensor polarization is no longer negligible (Fig. 2). Above this point the scattering becomes more strongly energy-dependent and is dominated by the 4.6-Mev resonance.

Our notation follows that of Stapp.[6] If $\vec{k}$ and $\vec{k}'$ are initial and final relative deuteron momenta, we define unit vectors $\vec{N}$, $\vec{K}$, and $\vec{Q}$ in the directions $\vec{k}\times\vec{k}'$, $\vec{k}'-\vec{k}$, and $\vec{k}'+\vec{k}$, respectively. Then if S_i ($i=1,2,3$) are the components of the spin-1 operator, the vector polarization $P_i \equiv \langle S_i \rangle$ and tensor polarization $T_{ij} \equiv \langle \frac{1}{2}(S_iS_j+S_jS_i) - \frac{2}{3}\delta_{ij} \rangle$ set up in the scattering of initially unpolarized deuterons have the forms

$$P_i = \beta N_i, \tag{1}$$

$$T_{ij} = \eta(N_iN_j - \tfrac{1}{3}\delta_{ij}) + \kappa(Q_iQ_j - K_iK_j) + \tau(Q_iK_j + K_iQ_j). \tag{2}$$

The analyzing power of the scattering is described by vector and tensor "analyzabilities" $\hat{P}_i$ and $\hat{T}_{ij}$,

$$\hat{P}_i = P_i, \tag{3}$$

$$\hat{T}_{ij} = T_{ij} - 2\tau(Q_iK_j + K_iQ_j), \tag{4}$$

such that the cross section σ for scattering polarized deuterons is

$$\sigma = \sigma_0(1 + \tfrac{3}{2}P_i\hat{P}_i + 3T_{ij}\hat{T}_{ij}). \tag{5}$$

Here P_i and T_{ij} describe the incident polarization and σ_0 is the unpolarized cross section. For pure vector polarization, this is like the familiar scattering of spin-$\frac{1}{2}$ particles, except for the factor $\frac{3}{2}$ in Eq. (5).

---

[1]L. J. B. Goldfarb, Nuclear Phys. 7, 622 (1958).
[2]L. J. B. Goldfarb and J. R. Rook, Nuclear Phys. (to be published).
[3]L. G. Pondrom, Phys. Rev. Letters 2, 346 (1959).
[4]Galonsky, Willard, and Welton, Phys. Rev. Letters 2, 349 (1959).
[5]A. Galonsky and M. T. McEllistrem, Phys. Rev. 98, 590 (1955).
[6]H. P. Stapp, thesis, University of California Radiation Laboratory Report UCRL-3098, 1955 (unpublished).

$_{\Lambda}H^{4}$ HYPERFRAGMENT EMITTED FROM AN ANTIPROTON CAPTURE STAR*

A. G. Ekspong, Å. Frisk, and B. E. Ronne
Institute of Physics, Uppsala, Sweden
(Received June 18, 1959)

The observation of a definite case of Λ^0 hyperon emission from an antiproton annihilation in a medium heavy nucleus is reported. The lambda hyperon is emitted bound in a $_{\Lambda}H^{4}$ hyperfragment.

It is known[1-7] that antiproton annihilations, in general, produce a number of pions and that strange particles occur only rarely. From emulsion experiments, Chamberlain et al.[5] estimate that about 3.5% of all antiproton stars contain $K\bar{K}$ meson pairs. A similar result has been obtained in our study. When the annihilation takes place in a nucleus, one may expect some cases where hyperons are produced, either by a secondary process involving the reabsorption of a $\bar{K}$ meson or by a primary process involving two nucleons and the antiproton. Observations of two possible Σ hyperons emitted from antiproton capture stars have been published.[1,5] In view of the uncertainties attached to these earlier observations, we regard our observation to be of some general interest.

The event occurred in an emulsion stack exposed to a beam of 740-Mev/c antiprotons at the Bevatron in Berkeley. The number of antiprotons observed in this experiment is 374. Details on the scanning technique and the identification of the antiprotons have been published elsewhere.[8]

A microphotograph of the antiproton star with the hyperfragment is shown in Fig. 1. The particle which is assigned to be the antiproton was found to be moving towards the star and to have protonic mass. As the kinetic energy of this particle at the star is only 96 ± 6 Mev and the energy release is at least 979 Mev, it is clear that the star represents the annihilation of an antiproton. All the tracks connected with this event are completely contained in the stack. Each of the eleven outgoing tracks are numbered as seen in the figure. Number 7, which according to our measurements most probably is a proton of 150-Mev energy, interacts in flight. All other particles come to rest.

Number 2 is the hyperfragment. This track is very suitably located for accurate measurements. It is 3630 microns long and passes through 3 plates before decaying at rest (at point B in the figure). The charge of the fragment was measured by counting the number of δ rays along the entire track length. The result $Z = 1$ is certain. The mass was determined by the constant sagitta scattering method to be 4.0 ± 1.1 proton masses. Calibration results from measurements on protons were utilized for both the charge and the mass determination. These results indicate that the particle is probably a H^3 or H^4 hyperfragment.

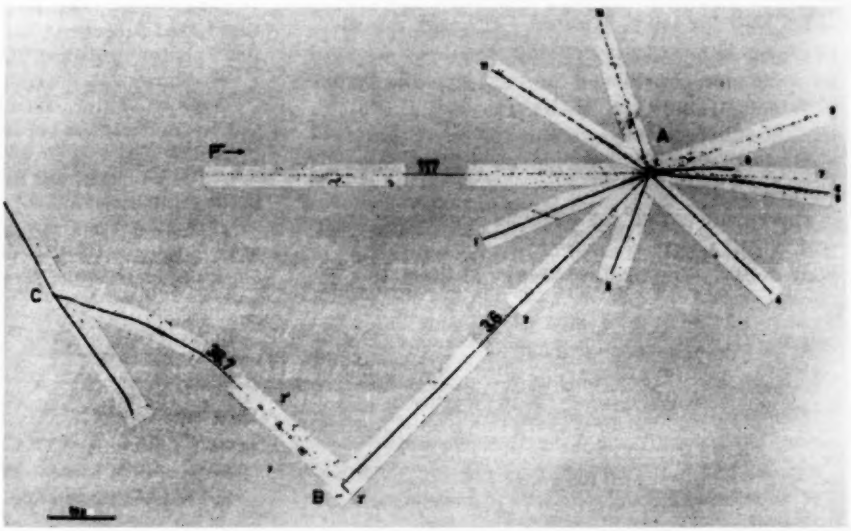

FIG. 1. Microphotograph of the antiproton annihilation at A and the mesonic decay of the $_{\Lambda}H^{4}$ fragment at B. The kinetic energy of the hyperfragment is 54 Mev. Path lengths are in millimeters. Track 10 is due to an 18-Mev negative π meson, track 11 to an 89-Mev He nucleus. All other prongs in star A represent protons.

The two secondary tracks, one of which is a negative pion, are collinear within experimental errors. They are emitted at an angle of 22.5° with the emulsion plane (in unprocessed emulsion). The range of the secondary π^- meson is 38.7 mm and it gives an absorption star at rest (at point C in the figure). The kinetic energy of the pion is then 52.3 ± 1.0 Mev, where the standard error is computed from straggling error, observational error, uncertainty of emulsion density, and uncertainty of shrinkage factor. The other secondary has a range of (8.0 ± 0.4) μ. The approximate collinearity of the two secondary prongs suggests that the event represents a two-body decay. We assume that this is the correct interpretation and will later return to a discussion of this assumption. The nature of the recoil particle is deduced from its observed range and its momentum, which is equal to the observed π-meson momentum on the above-mentioned assumption of a two-body decay. On the basis of momentum, we expect the range to be 8.0 ± 0.4 μ if the recoil particle is He^4, and 11.5 ± 0.5 μ if He^3. The measured range of 8.0 ± 0.4 μ is consistent with a He^4 recoil. This leads to the following interpretation of the event:

$$ {}_{\Lambda}H^4 \rightarrow He^4 + \pi^- + Q, $$

where $Q = 54.6 \pm 1.0$ Mev.

Other interpretations of this event were considered. In addition to the above elimination of a He^3 recoil because of range, it is further ruled out in a two-body decay, ${}_{\Lambda}H^3 \rightarrow He^3 + \pi^- + Q$, because it leads to a negative binding energy of -12.5 Mev for the Λ hyperon. Although the observed collinearity indicates a two-body decay, we have also considered the only possible three-body decay, namely ${}_{\Lambda}H^4 \rightarrow He^3 + n + \pi^- + Q$. This, too, is ruled out because it leads to a negative binding energy of the Λ hyperon (in this case $B_{\Lambda} < -15.7$ Mev).

The result is that the event is consistent only with a ${}_{\Lambda}H^4$ fragment undergoing mesonic two-body decay. The binding energy of the Λ in ${}_{\Lambda}H^4$ is then $B_{\Lambda} = 2.6 \pm 1.0$ Mev, which is consistent also with other measurements of this quantity.[9] In our calculation of the Λ-binding energy, we used the following input data: $Q_{\Lambda} = 37.36$ Mev, and proton separation energy in $He^4 = 19.80$ Mev.

A limited search for a neutral K meson in association with the event was undertaken. None was found in a volume such that the probability to find the decay of θ_1 meson was about 5%.

We conclude that the observation establishes the emission of a Λ hyperon bound in a ${}_{\Lambda}H^4$ fragment from an antiproton annihilation in a medium heavy nucleus. The binding energy of the hyperon in ${}_{\Lambda}H^4$ is 2.6 ± 1.0 Mev.

We are greatly indebted to Dr. E. J. Lofgren, Professor G. Goldhaber, Professor E. Segrè, Professor O. Chamberlain, and others at the Bevatron for arranging the exposure. We would like to thank Professor K. Siegbahn for his support and encouragement of this work. The support given by the Swedish Atomkommitté is gratefully acknowledged.

---

*This work is partly sponsored by the Air Research and Development Command through its European Office.

[1] Barkas, Birge, Chupp, Ekspong, Goldhaber, Goldhaber, Heckman, Perkins, Sandweiss, Segrè, Smith, Stork, Van Rossum, Amaldi, Baroni, Castagnoli, Franzinetti, and Manfredini, Phys. Rev. 105, 1037 (1957).

[2] Amaldi, Castagnoli, Ferro-Luzzi, Franzinetti, and Manfredini, Nuovo cimento 5, 1797 (1957).

[3] Ekspong, Johansson, and Ronne, Nuovo cimento 8, 84 (1958).

[4] A. H. Armstrong and G. M. Frye, Bull. Am. Phys. Soc. 2, 379 (1957).

[5] Chamberlain, Goldhaber, Jauneau, Kalogeropaulos, Segrè, and Silberberg, University of California Radiation Laboratory Report UCRL-8424, 1958 (unpublished).

[6] E. Segrè et al. (private communication).

[7] Horwitz, Miller, Murray, and Tripp, University of California Radiation Laboratory Report UCRL-8591 (unpublished).

[8] A. G. Ekspong and B. E. Ronne, Nuovo cimento (to be published).

[9] 1958 Annual International Conference On High-Energy Physics at CERN, edited by B. Ferretti (CERN Scientific Information Service, Geneva, 1958), p. 169.

ELECTRIC POLARIZABILITY OF THE NEUTRON*

L. L. Foldy
Case Institute of Technology, Cleveland, Ohio
(Received June 15, 1959)

Interest has recently developed in the subject of the electric polarizability of the neutron.[1,2] This is a quantity which can presumably be calculated when one has available sufficient knowledge of the structure of the neutron, in particular, its mesonic structure. Estimates of the polarizability based on current meson theory or on photomeson production data suggest a value lying between 4×10^{-43} cm^3 and 2×10^{-42} cm^3, while currently available experiments only place an upper limit of about 10^{-41} cm^3 on its value.

It is of some interest to remark that the mere existence of an anomalous (Pauli) moment for the neutron already implies a negative electric polarizability for the neutron, in a manner somewhat analogous to the situation for the neutron-electron interaction.[3] This may be seen by simply writing the Dirac Hamiltonian for a neutron with a Pauli moment μ_n in a uniform static external electric field $\vec{E}$:

$$H=\beta Mc^2+c\vec{\alpha}\cdot\vec{p}+i\mu_n\beta\vec{\alpha}\cdot\vec{E}.$$

Since $\vec{p}$ commutes with the Hamiltonian we can find the eigenvalues of the energy W for states in which $\vec{p}=0$:

$$H\psi=(\beta Mc^2+i\mu_n\beta\vec{\alpha}\cdot\vec{E})\psi=W\psi.$$

Then, since

$$H^2\psi=(M^2c^4+\mu_n{}^2E^2)\psi=W^2\psi,$$

one has immediately that the energy eigenvalues are

$$W=\pm[M^2c^4+\mu_n{}^2E^2]^{1/2}=\pm[Mc^2+\mu_n{}^2E^2/2Mc^2\cdots],$$

demonstrating an electric polarizability of

$$\alpha=-\mu_n{}^2/Mc^2=-6.2\times10^{-44}\ \text{cm}^3.$$

While this is somewhat smaller than anticipated contributions from the polarizability of the meson cloud, it is questionable whether it should therefore be dismissed lightly. It need only be remembered that the Pauli moment contribution to the neutron-electron interaction was also expected[3] to be small compared to the intrinsic interaction arising from the meson cloud, yet experiments have shown it to dominate the observed interaction for reasons still unfathomed.

It is interesting that should the intrinsic polarizability of the meson cloud indeed be anomalously small, the resultant polarizability of the neutron may be negative, a result which we believe not to have been anticipated. While it is easy to trace the negative sign of the magnetic contribution to the contribution of negative energy states in the one-particle theory, we have not been able to construct a rationalization in terms of classical or semiclassical concepts.

---

*Research supported by the U. S. Atomic Energy Commission.

[1] I. Aleksandrov and I. Bondarenko, J. Exptl. Theoret. Phys. U.S.S.R. 31, 726 (1956)[translation: Soviet Phys. JETP 4, 612 (1957)]; Barashenkov, Stakhanov, and Aleksandrov, J. Exptl. Theoret. Phys. U.S.S.R. 32, 154 (1957) [translation: Soviet Phys. JETP 5, 144 (1957)]; I. Aleksandrov, J. Exptl. Theoret. Phys. U.S.S.R. 33, 294 (1957) [translation: Soviet Phys. JETP 6, 228 (1958)].

[2] R. M. Thaler, Phys. Rev. 114, 827 (1959); G. Breit and M. L. Rustgi, Phys. Rev. 114, 830 (1959). We are indebted to Dr. Thaler for a prepublication copy of his manuscript.

[3] L. L. Foldy, Revs. Modern Phys. 30, 471 (1958) and references contained therein.

PROTON POLARIZATION IN MULTIPLE PION PRODUCTION AS A CONSEQUENCE OF THE ISOBAR MODEL*

L. F. Landovitz and L. Marshall†
Brookhaven National Laboratory, Upton, New York
(Received June 24, 1959)

The isobar model[1,2] for the system $p+\pi^+$ is in reasonable accord with the gross features of the momentum distribution for pions emitted in pion production in proton-proton collisions, and also in photoproduction of pions from nucleons. In the present note we shall show some consequences which follow near threshold for production of the isobar by pions if the model is taken seriously, i.e., the isobar production is assumed to be the dominant inelastic process.

We consider the process $\pi^+ + p \rightarrow \pi + N^*$, followed by $N^* \rightarrow \pi + N$. The isobar N^* is in a pure state $T=\frac{3}{2}$, $J=\frac{3}{2}$, positive parity. Because the initial system $\pi^+ + p$ is in a pure $T=\frac{3}{2}$ state, we need not consider any $T=\frac{1}{2}$ states. In Table I are shown the relevant angular momenta for initial and final configurations. From these it follows that

Table I. Possible angular momentum and parity states.

Orbital angular momentum of incident state l	Total angular momentum J	Orbital angular momentum of final state L	Parity
0	1/2	2	(-)
1	3/2, 1/2	1	(+)
2	5/2, 3/2	2, 0	(-)

if d and higher angular momenta are not excited in the incident configuration of $\pi^+ + p$, and if the final configuration has low energy, then only the $P_{3/2}$ and $P_{1/2}$ angular momentum states can be excited in the configuration $N^* + \pi$. With these assumptions, the production process $\pi + p \rightarrow N^* + \pi$ may be described by only two amplitudes a_3 and a_1 corresponding to the states $P_{3/2}$ and $P_{1/2}$.

We assume that the mass of the isobar corresponds to the peak of the p resonance. Of course, because of the width of the resonance, it is possible to produce the isobar at somewhat lower energies. The laboratory kinetic energy of the incident pion able to produce an isobar of this mass is 380 Mev; however, in practice, in order to obtain significant production one would use pions of somewhat higher energy. The cross section[3] for inelastic processes in πp scattering remains relatively small, ~3.6 mb, as compared with the total cross section, ~16 mb, at 400 Mev, from which one concludes that s and p waves alone are adequate to explain the magnitude of inelastic processes. Consequently it is reasonable to neglect d waves[4] in the initial system $p+\pi^+$. In the final system the particles are moving so slowly that d wave is ruled out here also.

In the case in which the isobar decay products are emitted in the production plane, the spin of the decay proton can be polarized[2] only perpendicular to this plane. We calculate its magnitude here in terms of the center-of-mass angles θ_1 and θ_2, where θ_1 is the angle between the momentum vectors of the pions involved in the production of the isobar and where θ_2 is the angle between the momentum of the pion produced by decay of the isobar and the incident direction. In what follows, we have disregarded the small change in θ_2 caused by the transformation from the rest system of the isobar to the barycentric system for production.

The amplitude for the production process $\pi^+ + p \rightarrow N^* + \pi$ was written in terms of a_3 and a_1, the partial amplitudes for $J=\frac{3}{2}$ and $J=\frac{1}{2}$, respectively, assuming the Z axis to be along the momentum vector of the incident pion.

$$f(\theta,\varphi) = 6^{\frac{1}{2}} \mathcal{Y}_{3/2,1}{}^{1/2} a_3 - \sqrt{3}\, \mathcal{Y}_{1/2,1}{}^{1/2} a_1.$$

This expression was re-analyzed into states of the isobar of spin $\frac{3}{2}$, and of the associated pion. The isobar then was assumed to decay into a $\pi+N$; correspondingly the isobar wave functions were rewritten in terms of wave functions for the final π, N system. Finally the spin functions for the final proton were projected onto an axis perpendicular to the scattering plane, which is here taken to be the y axis. For events in which all particles lie in the scattering plane, azimuthal angle $\varphi_1 = \varphi_2 = 0$ where subscripts 1 and 2 are as before, we find the polarization of the decay proton to be given by the expression

$$P(\theta_1,\theta_2) = i\tfrac{2}{5} \frac{(a_1 a_3^* - a_3 a_1^*)}{\sigma(\theta_1,\theta_2)} [6\cos\theta_1 \sin\theta_1 \cos^2\theta_2 + 9\sin^2\theta_1 \cos\theta_2 \sin\theta_2 - 3\cos\theta_1 \sin\theta_1 \sin^2\theta_2],$$

where $\sigma(\theta_1, \theta_2)$ is given by

$$\sigma(\theta_1, \theta_2) = |a_1|^2[3(\cos^2\theta_1\cos^2\theta_2 + \sin^2\theta_1\sin^2\theta_2) + 1 + 6\cos\theta_1\cos\theta_2\sin\theta_1\sin\theta_2]$$
$$+ \tfrac{2}{5}|a_3|^2[1 + 3\cos^2\theta_1\cos^2\theta_2 + 15\sin^2\theta_1\cos^2\theta_2 - 12\cos\theta_1\cos\theta_2\sin\theta_1\sin\theta_2]$$
$$+ (\tfrac{2}{5})^{\frac{1}{2}}(a_1a_3^* + a_3a_1^*)[4\cos^2\theta_1\cos^2\theta_2 - 3\cos\theta_1\sin\theta_1\cos\theta_2\sin\theta_2 - 2\sin^2\theta_1\sin^2\theta_2$$
$$+ \cos^2\theta_1\sin^2\theta_2 + 4\sin^2\theta_1\cos^2\theta_2] .$$

A significant consequence of this model is that the protons are not polarized for certain values of the angles θ_1 and θ_2. Figure 1 shows the correlation of θ_1 and θ_2 for those values which give zero polarization. Of course the experimentally observed polarization will not be exactly zero at these angles because of the background direct or nonisobaric production of $\pi+\pi+N$. But if the model has validity, then the polarization should be low or minimal in the regions indicated in Fig. 1. Furthermore, it may be seen by inspection of the expression for the polarization that its relative sign is different on opposite sides of the lines of zero polarization. It may be mentioned that there exist configurations of isobar production by $\pi^+ + p$ such that the directly produced pion can be readily distinguished from the decay pion by its angle of emission provided that the angle and energy of the decay proton is measured.

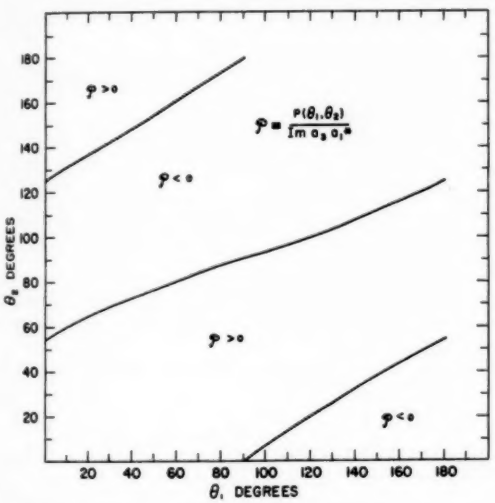

FIG. 1. Contour diagram of polarization.

We wish to thank R. Serber, G. C. Wick, C. N. Yang, T. D. Lee, and M. Goldhaber for helpful conversations.

*Work performed under the auspices of the U. S. Atomic Energy Commission.

†On leave of absence from University of Chicago, Chicago, Illinois.

[1]M. Gell-Mann and K. M. Watson, Annual Review of Nuclear Science (Annual Reviews, Inc., Palo Alto, 1954), Vol. 4, p. 219. D. C. Peaslee, Phys. Rev. 94, 1085 (1954); 95, 1580 (1954). N. Austern, Phys. Rev. 100, 1522 (1955). R. Sternheimer and S. Lindenbaum, Phys. Rev. 109, 1727 (1958).

[2]Saul Barshay, Phys. Rev. 111, 1651 (1958).

[3]S. M. Korenchenko and V. G. Zinov, Proceedings of the Padua-Venice Conference on Mesons and Recently Discovered Particles, 1957 (unpublished), p. X-23.

[4]Blevins, Block, and Leitner, Phys. Rev. 112, 1287 (1958); W. J. Willis, Phys. Rev. (to be published).

VARIATIONAL PRINCIPLE FOR GEOMETRODYNAMICS

David Sharp
Palmer Physical Laboratory, Princeton University, Princeton, New Jersey
(Received June 23, 1959)

The purpose of this note is to propose a variational principle for geometrodynamics, to derive from it certain of the field equations, and to relate the problem of obtaining the remaining field equations to the problem of finding a superpotential for the metric tensor.

Misner and Wheeler,[1] following Rainich,[2] have shown that the content of general relativity and classical source-free electromagnetism can be fully expressed in terms of quantities depending only on the metric tensor $g_{\mu\nu}$ of a Riemannian space. In their formulation the field equations, fully equivalent to the usual ones, are

$$R_{\mu\alpha}R^{\alpha}{}_{\nu}=g_{\mu\nu}(R_{\alpha\beta}R^{\alpha\beta})/4, \tag{1}$$

$$R_{\mu}{}^{\mu}=R=0, \tag{2}$$

$$R_{00}\geq 0, \tag{3}$$

$$\alpha_{\beta|\gamma}-\alpha_{\gamma|\beta}=0, \tag{4}$$

where the vector α_β is defined as

$$\alpha_{\beta}=(-g)^{1/2}[\beta\lambda\mu\nu]R^{\lambda\gamma|\mu}{}_{\gamma}{}^{\nu}/R_{\sigma\tau}R^{\sigma\tau}. \tag{5}$$

For some purposes it is useful to replace the $10+1=11$ equations (1) and (2) by the equivalent 10 equations:

$$\text{“}-\tfrac{1}{2}\text{”}g_{\mu\nu}R-\frac{R_{\mu\alpha}R^{\alpha}{}_{\nu}}{(R_{\sigma\tau}R^{\sigma\tau})^{1/2}}+\tfrac{1}{4}g_{\mu\nu}(R_{\sigma\tau}R^{\sigma\tau})^{1/2}=0. \tag{6}$$

The identity of (6) to (1) and (2) may be seen by setting $\mu=\nu$ and summing. The factor $-\frac{1}{2}$ could just as well have any other constant value—hence the quotes.

By way of explanation it may be recalled that the curl condition (4) guarantees the existence of a scalar,

$$\alpha(x)=\int_{0}^{x}\alpha_{\beta}dx^{\beta}+\alpha_{0}, \tag{7}$$

the "complexion" of the electromagnetic field. If $\alpha=n\pi$ $(n=0,1,2,\ldots)$, we have a pure electric field; if $\alpha=\frac{1}{2}n\pi$ $(n=1,3,\ldots)$, the field is pure magnetic. The complexion at a point, together with the value of the Ricci curvature tensor at the point, completely determine the electromagnetic field $f_{\mu\nu}$, and hence also the stress-energy tensor,

$$T_{\mu\nu}=f_{\mu\alpha}f^{\alpha}{}_{\nu}-\tfrac{1}{4}g_{\mu\nu}f_{\sigma\tau}f^{\sigma\tau}, \tag{8}$$

at that point.

The algebraic equations (1)-(3) satisfied by the Ricci curvature express the two-way connection between the electromagnetic field tensor $f_{\mu\nu}$ and the Ricci tensor $R_{\mu\nu}$. Thus, any electromagnetic field tensor $f_{\mu\nu}$ produces a Ricci curvature $R_{\mu\nu}$ that satisfies (1)-(3). Conversely, given an $R_{\mu\nu}$ that satisfies (1)-(3), we can solve for $f_{\mu\nu}$, the solution being uniquely determined except for α. The curl condition (4) subsequently determines α up to an additive constant α_0.

It is often very helpful to have a variational formulation of a set of field equations.

Such a formulation is well known[3,4] in the more familiar version of general relativity plus electromagnetism, where the $f_{\mu\nu}$ are treated as foreign objects immersed in the metric space rather than expressed—as above in Eqs. (1)-(5)—directly in purely geometric terms.

In the traditional version of general relativity plus electromagnetism, the coupled field equations are

$$R_{\mu\nu}-\tfrac{1}{2}g_{\mu\nu}R=f_{\mu\alpha}f^{\alpha}{}_{\nu}-\tfrac{1}{4}g_{\mu\nu}f_{\sigma\tau}f^{\sigma\tau}, \tag{9}$$

$$f^{\mu\nu}{}_{|\nu}=0, \tag{10}$$

$${}^{*}f^{\mu\nu}{}_{|\nu}=0. \tag{11}$$

The variational formulation of these equations has the form

$$\delta I=0,\quad I=\int\mathfrak{L}\,d\tau,\quad d\tau=dx^{0}dx^{1}dx^{2}dx^{3}, \tag{12}$$

with

$$\mathfrak{L}=\text{(Lagrangian density for the gravitational field)}+\text{(Lagrangian density for electromagnetic field)} \tag{13}$$

$$=R(-g)^{1/2}+\tfrac{1}{2}(-g)^{1/2}f_{\sigma\tau}f^{\sigma\tau}. \tag{14}$$

The usual procedure to obtain the field equa-

tions from the above is to require (for detail, see references 3 and 4):

(a) The existence of a vector 4-potential for $f_{\mu\nu}$:

$$f_{\mu\nu}=\varphi_{\mu|\nu}-\varphi_{\nu|\mu} \quad \text{or} \quad f^{\mu\nu}{}_{|\nu}=0; \tag{15}$$

(b) $f_{\mu\nu}$ (or φ_μ) and $g^{\mu\nu}$ are treated as the quantities to be varied;

(c) $\delta\varphi_\mu$ and $\delta g^{\mu\nu}$ are both to vanish on the surface σ bounding τ.

We propose for geometrodynamics the Lagrangian density

$$\mathfrak{L}=R(-g)^{1/2}-\tfrac{1}{2}(-g)^{1/2}(R_{\mu\nu}R^{\mu\nu})^{1/2} \times\cos 2\left[\int_0^x \alpha_\beta dx^\beta\right]. \tag{16}$$

The first term is, as before, the Lagrangian density for the gravitational field. Likewise, the second term is an expression for the Lagrangian density E^2-H^2 for the electromagnetic field, expressed in purely geometrical form. This expression can be derived from results in Misner and Wheeler.[5]

We see that our Lagrangian density is a functional of the metric tensor $g^{\mu\nu}$ and its derivatives up to the second order, and of the path of integration π occurring in the definition of $\alpha(x)$, Eq. (7).

We require that $I=\int\mathfrak{L}d\tau$ be stationary with respect to arbitrary variations of both the path π and $g^{\mu\nu}$.

We first vary with respect to π. $\delta_\pi I=0$ results in the condition that the integral

$$\int_0^x \alpha_\beta dx^\beta, \tag{17}$$

be independent of the path from 0 to x. This will be true if the integrand α_β has a vanishing curl:

$$\alpha_{\beta|\gamma}-\alpha_{\gamma|\beta}=0. \tag{4}$$

This is one of the equations we seek. We may now write $\mathfrak{L}$ in a slightly simpler form:

$$\mathfrak{L}=R(-g)^{1/2}-\tfrac{1}{2}(R_{\mu\nu}R^{\mu\nu})^{1/2}\cos 2\alpha. \tag{18}$$

With no loss of generality we can set $\alpha(x)=0$ at the point of variation, since this amounts to nothing more than choosing a convenient origin of coordinates. Note, however, that this does not imply that $\delta\alpha=0$, although $\delta(\cos 2\alpha)=0$.

At this point it would seem natural (1) to vary Eq. (18) with respect to $g^{\mu\nu}$, (2) to integrate by parts terms containing derivatives of $\delta g^{\mu\nu}$, and (3) to set equal to zero the resulting coefficient of $\delta g^{\mu\nu}$. The field equations obtained in this way are not satisfactory; they are not equivalent to the desired and expected Eq. (6).

It seems reasonable to attribute this difficulty to a wrong choice of the quantities to hold fixed on the surface, not to a wrong choice of quantities to be varied.

This is not the first time that such a problem has arisen, as witness the variational principle:

$$\delta\int(E^2-H^2)d(\text{vol})=\delta\int(-g)^{1/2}f_{\mu\nu}g^{\mu\alpha}g^{\nu\beta}f_{\alpha\beta}d\tau=0, \tag{19}$$

for electromagnetism alone in a space with prescribed metric $g_{\mu\nu}$.

The most primitive analysis of this variational principle, based on the assumption that the $f_{\mu\nu}$ are the quantities to be varied, and that the variations of $f_{\mu\nu}$ vanish at the boundaries, leads to the incorrect result that $f_{\mu\nu}=0$ throughout the interior.

The customary procedure is to add a supplementary condition, Eq. (15), and treat the φ_μ as the quantities to be varied, and hold them fixed on the boundary.

By setting the coefficient of $\delta\varphi_\mu$ equal to zero, we obtain four of Maxwell's equations. The other four were assumed from the outside, Eq. (15).

However, there is still a third approach,[6-9] due to Finzi, whereby one can obtain all eight of Maxwell's equations without the addition of such a subsidiary condition from outside.

Finzi begins by observing that any antisymmetric tensor $f_{\mu\nu}$ can be expressed in the form

$$f_{\mu\nu}=A_{[\mu|\nu]}+\frac{(-g)^{1/2}[\mu\nu\alpha\beta]g^{\mu\alpha}g^{\nu\beta}B_{[\alpha|\beta]}}{2}, \tag{20}$$

where A_μ and B_α are 4-vectors. We now vary the action integral with respect to both A_μ and B_α, subject to the condition that they both be fixed on the boundary. The demand that the action be stationary immediately produces all eight of Maxwell's equations.

Judging by the analogy between the $f_{\mu\nu}$ as field variables in electromagnetism and the $g^{\mu\nu}$ as field variables in gravitation, we expect that there are alternative ways to vary arbitrarily the field variables within a space-time region. The ways differ from each other in the choice of quantities kept fixed on the 3-surface bounding this region.

It was wrong in electromagnetism to think of the $f_{\mu\nu}$ as fixed on the surface. It appears equally wrong in geometrodynamics to think of the $g^{\mu\nu}$ as fixed on the surface.

In electromagnetism we know the potentials which should be fixed on the surface. In geometrodynamics we do not yet know these potentials.

Therefore, we regard the problem ahead as not to change the variational principle Eq. (16), which is so plausible on physical grounds, but rather to find the right superpotential in terms of which to express the $g^{\mu\nu}$.

In discussions (1) of the quantization of general relativity and (2) of the "true variables" of general relativity, the hope has often been expressed to find these superpotentials. We now have a third and perhaps even stronger motive to construct these quantities: to validate—if possible—a variational principle which, for the first time, summarizes in purely geometrical terms the whole content of classical source-free electromagnetism and general relativity.

I am deeply grateful to Professor D. C. Spencer, and especially to Professor J. A. Wheeler, for many long and helpful discussions on this problem.

[1]C. W. Misner and J. A. Wheeler, Ann. Phys. 2, 525 (1957).
[2]G. Y. Rainich, Trans. Am. Math. Soc. 27, 106 (1925).
[3]V. Bargmann, Revs. Modern Phys. 29, 161 (1957).
[4]W. Pauli, Theory of Relativity (Pergamon Press, New York, 1958).
[5]See reference 1, pp. 538-540, 544.
[6]B. Finzi, Atti accad. nazl. Lincei. Rend., Classe sci. fis. mat. e nat. 12, 378, 477 (1952).
[7]J. A. Wheeler, "Notes and Queries on the Spacelike Description of Geometrodynamics," 1959 (unpublished).
[8]J. L. Synge, Relativity: the Special Theory (North-Holland Publishing Company, Amsterdam, 1956).
[9]A. M. Pratelli, Ann. scuola normale superiore Pisa, sci. fis. mat. 7, 161 (1953).

POSSIBLE METHODS FOR THE DETERMINATION OF STRANGE-PARTICLE PARITIES*

A. Sirlin and R. Spitzer†
Physics Department, Columbia University, New York, New York
(Received June 16, 1959)

The question of the intrinsic parities of the strange particles has been extensively discussed in the past. The aim of this note is to point out two possible experiments that may shed light on this matter.

We first consider the capture reaction

$$K^- + d \to Y + N. \tag{1}$$

It has been recently suggested that the capture of K^- in liquid hydrogen and deuterium occurs predominantly from bound s states.[1] In this note we shall consider that statement as a working hypothesis and shall derive a theorem that may be used to obtain information regarding the parity of the K meson relative to the YN system. With the assumption that K capture occurs predominantly from s states (bound or from the continuum) relative to the center of mass of the deuteron, the most general form of the transformation matrix in spin space is

$$M = [a + b(\vec{\sigma}_1\cdot\vec{k})(\vec{\sigma}_2\cdot\vec{k})]T \quad \text{for scalar } K, \tag{2a}$$

and

$$M = [c\vec{\sigma}_1\cdot\vec{k} + d\vec{\sigma}_2\cdot\vec{k}]T \quad \text{for pseudoscalar } K, \tag{2b}$$

where $\vec{k}$ is a unit vector along the direction of the relative momentum of the final system and T is the triplet projection operator. The operator T simply describes the spin correlation of the initial state. We also note that the other possible invariants $\vec{\sigma}_1\cdot\vec{\sigma}_2 T$ and $\vec{\sigma}_1\cdot(\vec{k}\times\vec{\sigma}_2)T$ can be reduced to the general forms given in Eqs. (2a) and (2b), respectively.

We now evaluate the correlation between the components of the spins of the Y and N along a direction $\vec{n}$, perpendicular to $\vec{k}$:

$$\langle\sigma_{1n}\sigma_{2n}\rangle = \mathrm{Tr}[MM^\dagger\sigma_{1n}\sigma_{2n}]/\mathrm{Tr}[MM^\dagger]. \tag{3}$$

Inserting expressions (2a) and (2b) into (3), we obtain

$$\langle\sigma_{1n}\sigma_{2n}\rangle = |a-b|^2/[|a+b|^2 + 2(|a|^2 + |b|^2)] \geq 0, \tag{4a}$$

and

$$\langle\sigma_{1n}\sigma_{2n}\rangle = -|c-d|^2/[|c+d|^2 + 2(|c|^2 + |d|^2)] \leq 0, \tag{4b}$$

for scalar and pseudoscalar K, respectively.

Thus, the K parity can be determined, in principle, by the measurement of the sign of this correlation.

The determination of $\langle \sigma_{1n}\sigma_{2n}\rangle$ in reaction (1) presents two main practical difficulties: in the first place, reaction (1) occurs only in about 1% of all K^- capture reactions; secondly, if the final system is Λn, this measurement will involve the determination of the spin direction of n, which may present special problems. The spin direction of the Λ may be determined from the angular distribution of the decay products. If the final system is $\Sigma^- p$, the determination of the spin direction of the Σ^- may be difficult because of the apparently small value of the asymmetry parameter in Σ^- decay.

It is perhaps interesting to observe that if, in the more frequent reactions

$$K^- + d \to Y + N + \pi, \tag{5}$$

it turns out to be possible to isolate those events in which the Y and N are produced with sufficiently small relative momentum so that they are predominantly in a relative s state, then a similar theorem would hold for their spin correlation. In that case, in Eqs. (2a) and (2b) the vector $\vec{k}$ would represent the momentum of the pion relative to the YN system and the results of Eqs. (4a) and (4b) would be interchanged because of the pseudoscalar nature of the pion field. Reactions of type (5) have the advantage that they are more frequent than (1) and they would permit the investigation of the spin correlations of the Λp and the $\Sigma^+ n$ systems, which may avoid some of the difficulties mentioned above.

Finally we mention the reaction

$$\Sigma^\pm + \mathrm{He}^4 \to {}_\Lambda\mathrm{He}^5 + \pi^\pm, \tag{6}$$

as a possible means of determining the relative Λ-Σ parity. (We assume spin $\frac{1}{2}$ for ${}_\Lambda\mathrm{He}^5$.) When the Σ has a polarization $\vec{P}_0$, the differential cross section for reaction (6) is given by

$$d\sigma/d\Omega = (d\sigma/d\Omega)_0 (1 \pm \vec{P}_0 \cdot \vec{P}_1), \tag{7}$$

where $\vec{P}_1$ is the polarization of the ${}_\Lambda\mathrm{He}^5$ in the case $\vec{P}_0 = 0$ and $(d\sigma/d\Omega)_0$ is the corresponding differential cross section. The +(-) sign in Eq. (7) applies in the case in which the relative intrinsic parity of the initial and final systems is even (odd). Thus, the relative intrinsic parity of the final and initial systems in (6) can be determined, in principle, by a measurement of $\vec{P}_1$ and the left-right asymmetry for $\vec{P}_0 \neq 0$. The derivation of Eq. (7) follows the same lines as the theorems recently given by Bilenky[2] and Bohr.[3]

The authors wish to thank J. Franklin, N. Kroll, B. Margolis, and J. Steinberger for useful conversations.

*This work was supported by the U. S. Atomic Energy Commission.

†Address after summer 1959: Department of Physics, Purdue University, Lafayette, Indiana.

[1]Day, Snow, and Sucher, Phys. Rev. Letters 3, 61 (1959).

[2]S. M. Bilenky, Nuovo cimento 10, 1049 (1958).

[3]A. Bohr, Nuclear Phys. 10, 486 (1959).

ELECTROMAGNETIC TRANSITIONS BETWEEN μ MESON AND ELECTRON*

S. Weinberg†
Columbia University, New York, New York

and

G. Feinberg‡
Brookhaven National Laboratory, Upton, New York

(Received June 15, 1959)

The existence of the ordinary μ decay, $\mu \to e + \nu + \bar{\nu}$, seems to prove that the muon and electron do not differ in any quantum numbers.[1] It follows that weak electromagnetic transitions between muons and electrons could occur, if there is a mechanism to produce them. For example, one such mechanism would exist if the μ decay was not caused by a direct $\bar{\mu}e\bar{\nu}\nu$ Fermi interaction but instead involved a virtual charged boson. This particular possibility seems ruled out, since the predicted[2] rate for $\mu \to e + \gamma$ would be considerably greater than the upper limit set by recent experiments.[3,4] The purpose of this note is to discuss phenomenologically (without

attachment to any specific mechanism) other kinds of electromagnetic transitions between muon and electron that may be possible even if $\mu \to e + \gamma$ is somehow suppressed.

Since muon and electron both have spin $\frac{1}{2}$, the general μ-e-γ interaction may be described by four form factors, which correspond roughly to distributions of $E0$, $M0$, $E1$, and $M1$ transition moments. They are defined by[5]

$$\langle e|J_\lambda(0)|\mu\rangle = -ie(2\pi)^{-3}\bar{u}_e\Big[f_{E0}(q^2)\Big(\gamma_\lambda + iq_\lambda\frac{m_\mu}{q^2}\Big) + f_{M0}(q^2)\Big(\gamma_5\gamma_\lambda + i\gamma_5\frac{q_\lambda m_\mu}{q^2}\Big) + f_{E1}(q^2)\gamma_5\sigma_{\lambda\eta}\frac{q^\eta}{m_\mu} + f_{M1}(q^2)\sigma_{\lambda\eta}\frac{q^\eta}{m_\mu}\Big]u_\mu. \quad (1)$$

Here J_λ is the electromagnetic current, and $q_\lambda = p_{e\lambda} - p_{\mu\lambda}$ is the momentum transfer. The form factors f_{E0}, f_{M0}, f_{E1}, f_{M1} are dimensionless functions of

$$q^2 = q_\lambda q^\lambda = -\vec{q}^2 + (q^0)^2.$$

Equation (1) follows from Lorentz invariance, current conservation, and the Dirac equations for u_e and u_μ, with the electron mass neglected.

In order to avoid an infinity in (1) for $q^2 \to 0$, we must have

$$f_{E0}(0) = 0, \quad f_{M0}(0) = 0. \quad (2)$$

Furthermore, if ϵ_λ is the polarization four-vector of a real photon with momentum $-q_\lambda$ ($q^2 = 0$), we must have $q_\lambda\epsilon^\lambda = 0$. We therefore have the familiar result that the $E0$ and $M0$ terms cannot contribute to the rate of emission of a real photon, which is given by

$$\omega(\mu \to e + \gamma) = m_\mu \alpha \xi_1^2,$$

$$\xi_1^2 = \tfrac{1}{2}[|f_{E1}(0)|^2 + |f_{M1}(0)|^2]. \quad (3)$$

Thus the observed absence of $\mu \to e + \gamma$ decay tells us nothing about the possible existence of an $E0$ or $M0$ form factor, or about the possibility that $f_{E1}(q^2)$ or $f_{M1}(q^2) \neq 0$, although $f_{E1}(0) = f_{M1}(0) = 0$.

Actually, because of the presumably "chiral" character of lepton interactions, it is not difficult to find examples of theories in which we expect that f_{E0} and f_{M0} would be much greater than f_{E1} and f_{M1}. Suppose, for instance, that in addition to the usual μ-decay Fermi interaction, the muon and electron also have a Fermi interaction of the form

$$H = g\bar{\psi}_e\gamma_\lambda(1+\gamma_5)\psi_\mu\bar{\psi}_f\gamma^\lambda(1+\gamma_5)\psi_f, \quad (4)$$

with some charged particle f.[6] This interaction will generate, through "vacuum polarization" type diagrams, monopole form factors given by

$$f_{E0}(q^2) = -f_{M0}(q^2) = -\frac{gq^2}{12\pi^2}\Big[\tfrac{5}{6} + D - V\Big(\frac{q^2}{4m_f^2}\Big)\Big], \quad (5)$$

where m_f is the mass of f, D is a logarithmically divergent constant, given in terms of a cutoff λ by

$$D = \ln\Big(\frac{m_f^2+\lambda^2}{m_f^2}\Big) + \frac{m_f^2}{m_f^2+\lambda^2} - 1, \quad (6)$$

and V is[7] the vacuum polarization function

$$-V(x) = \tfrac{5}{3} - \frac{1}{x} + \Big(1 - \frac{1}{2x}\Big)\Big(1 + \frac{1}{x}\Big)^{1/2}\ln\Big|\frac{(1+1/x)^{1/2}-1}{(1+1/x)^{1/2}+1}\Big| \to -\tfrac{4}{5}x \text{ as } x \to 0. \quad (7)$$

For example, if we take $q^2 = m_\mu^2$, and $\lambda = m_p$, then $f_{E0} = -f_{M0} = f$:

$$f = -g(m_\mu^2/12\pi^2)\times 4.4.$$

On the other hand, in this model f_{E1} and f_{M1} are of order ge^2, since a virtual photon must be emitted and absorbed to produce any dipole transition moment.[8] This is a direct consequence of the "chirality conservation" of the μ-e covariant in (4), and would still hold if the factor

$$\bar{\psi}_f\gamma^\lambda(1+\gamma_5)\psi_f$$

were replaced by a more complicated function of the f-field operators. It should be mentioned that, realistically, f could only be a muon if the coupling constant in (4) is comparable with the Fermi constant. This is because we must have $m_f > m_\mu/2$ in order to avoid the unobserved decay process $\mu \to e + f + \bar{f}$, and furthermore f can only interact weakly with nuclei in order to avoid the unobserved nuclear absorption process $\mu + N \to e + N'$ in amounts comparable to ordinary μ capture.

In order to test the possible existence of the $E0$ and $M0$ terms in (1) or of the $E1$ and $M1$ terms for $q^2 \neq 0$, it is necessary to consider cases where the $\mu \to e$ transition is accompanied by an interaction with a virtual photon.[8] For example, a μ^- bound in a $1S$ state around a nucleus N may

absorb a virtual photon from the Coulomb field of the nucleus, forming an electron and a recoiling nucleus N'. The kinematics of this will be almost identical to those in ordinary μ^- absorption, the electron and N' being emitted with opposite momenta of magnitude $m_\mu c = 106$ Mev/c, providing that the excitation of the nucleus is small.

The rate of such a transition is given by

$$\omega_{N\to N'} = 16 m_\mu Z_{\text{eff}}^4 \alpha^5 \xi_0^2 Z |F_{N'N}|^2, \quad (8)$$

where $F_{N'N}$ is defined by

$$\langle N'|J^0(0)|N\rangle = (2\pi)^{-3} Ze F_{N'N}(q^2), \quad (9)$$

and

$$\xi_0^2 = \tfrac{1}{2}[|f_{E0}(m_\mu^2) + f_{M1}(m_\mu^2)|^2 + |f_{M0}(m_\mu^2) + f_{E1}(m_\mu^2)|^2]. \quad (10)$$

[We are using a plane wave for the electron, a constant wave function for the muon, and take the density of states for the μ^- at the nucleus to be $Z_{\text{eff}}^4 \alpha^3 m_\mu^3/\pi Z$. Only virtual "timelike" photons are assumed to contribute. Terms of order m_μ/m_N or $(m_{N'} - m_N)/m_\mu$ are neglected throughout.]

For experimental purposes, it is best to compare (8) with the rate for ordinary μ^- absorption[9]:

$$\omega_{\text{abs}} \simeq (1/2\pi^2) Z_{\text{eff}}^4 \alpha^3 \xi_\beta^2 m_\mu, \quad (11)$$

$$\xi_\beta^2 = \tfrac{1}{2}(|C_V|^2 + |C_{V'}|^2 + 3|C_A|^2 + 3|C_{A'}|^2) m_\mu^4. \quad (12)$$

We have then

$$\omega_{N\to N'}/\omega_{\text{abs}} = 32\pi^2 \alpha^2 Z |F_{N'N}|^2 \xi_0^2/\xi_\beta^2 \simeq 0.017 Z |F_{N'N}|^2 \xi_0^2/\xi_\beta^2. \quad (13)$$

The matrix element (9) is just the Born approximation nuclear matrix element for electron scattering ($e + N \to e + N'$) at momentum transfer

$$(q^2)^{1/2} \simeq 2E_e \sin(\theta/2) = m_\mu. \quad (14)$$

The cross section for this process in Born approximation is

$$\left(\frac{d\sigma}{d\Omega}\right)_{\text{lab}} \simeq \frac{Z^2 \alpha^2 \cos^2(\theta/2) |F_{N'N}|^2}{4E_e \sin^4(\theta/2)}. \quad (15)$$

If the Born approximation gave a correct description of electron scattering, one could use the experimental data directly to compute the variation of $\omega_{N\to N'}/\omega_{\text{abs}}$ from nucleus to nucleus. Since the Born approximation is not accurate over the whole periodic table, it seems more reasonable to use the information obtained about nuclear charge distributions in the electron scattering experiments to compute $F_{N'N}$. For the elastic processes, where $N = N'$, we estimate F_{NN} using a "Fermi shape" for the nuclear charge density,[10] with radius $1.08 \times 10^{-13} A^{1/3}$ cm and surface thickness $t = 2.5 \times 10^{-13}$ cm. Then setting $(q^2)^{1/2} = 5.36 \times 10^{12}$ cm^{-1}, we obtain

$$F_{NN} = \frac{3}{\Theta^3} \frac{(1.10 \sin\Theta - 0.86\Theta\cos\Theta)}{1 + 0.916/\Theta^2}, \quad \Theta \equiv 0.579 A^{1/3}. \quad (16)$$

The factor $Z|F_{NN}|^2$ in (13) then reaches a maximum of about 6 for nuclei near Cu, falls off slowly for heavier elements to about 2.5 for Pb, where our approximations are not valid anyway, and falls off rapidly for lighter elements, where the shape probably differs from the Fermi shape anyway.

In addition to the coherent process where $N = N'$, we must also consider the possibility of inelastic processes, where N' is some excited state of N. Here we can make use of a theorem known in the study of muon and electron scattering.[11] We make the following assumptions: (1) Born approximation, (2) closure approximation, (3) neglect of structure and mesonic effects, and (4) neglect of nucleon-nucleon correlations in N, except for the Pauli principle. Then

$$\sum_{N' \neq N} |F_{N'N}|^2 \leq 1/Z, \quad (17)$$

so that

$$\sum_{N'} |F_{N'N}|^2 Z \leq 1 + Z|F_{NN}|^2. \quad (18)$$

This factor then reaches a maximum of about 7 for nuclei near Cu. Since the coherent process $N \to N$ occurs for such nuclei at least six times more frequently than all inelastic processes (providing the above assumptions are justified), the electron emitted will have a very sharp spectrum, peaked at 105 Mev.

It should be noted that the ordinary μ^- capture, which involves the change of a proton into a neutron, cannot lead to the same nucleus, and thus gets no contribution from the coherent process.

The best experimental evidence on possible electrons from μ capture was obtained for cop-

per.[12] This experiment showed that

$$\omega_{N\to N'}(\mathrm{Cu})/\omega_{\mathrm{abs}}(\mathrm{Cu}) < 5\times 10^{-4},$$

so that, taking 7 as the value of $\sum_{N'}|F_{N'N}|^2 Z$, we have

$$\xi_0^2/\xi_\beta^2 \lesssim 4\times 10^{-3}. \qquad (19)$$

This indicates the amount by which the μ-e-γ form factors must be reduced compared to the μ decay coupling on the basis of present experiments. For comparison, the intermediate vector boson theory gives an answer of the order of $\xi_0^2/\xi_\beta^2 \sim (1/64\pi^2)^2$ for this ratio. In view of the mysteries surrounding the relation between muons and electrons, a more intensive study of whether electrons come from μ capture would be desirable.

The experiment of Steinberger and Wolfe was performed to test the possible existence of μepp and μenn Fermi interactions. The ratio of $\mu + N \to e + N'$ to ordinary μ absorption would, for vector coupling of equal strength to p and n, be proportional to $\sum_{N'} A^2 |F_{N'N}|^2/Z$. According to our calculations, this factor is about equal to 30 for Cu. Since this enhancement factor was taken to be about 4 in reference 12, the sensitivity of that experiment as a test of equal μepp and μenn vector interactions is about 7 times better than quoted.

Another experimental test of $\mu \to e$ transitions involving virtual photons would be the internal conversion process $\mu \to e + (e^+ + e^-)$. The rate for this process depends in a complicated way on the form of the functions f_{E0}, f_{M0}, f_{E1}, f_{M1} since it does not take place at fixed momentum transfer. (We cannot use the approximation of Kroll and Wada[13] here, as was done in reference 2, since we are supposing that the decay $\mu \to e + \gamma$ does not occur.) An order-of-magnitude estimate gives

$$\omega(\mu \to 3e)/\omega(\mu \to e + \nu + \bar{\nu}) \sim (e^4/4)(\xi_0^2/C_V^2).$$

Experimentally,[14] this ratio is less than 10^{-5}, so that $\xi_0^2/\xi_\beta^2 \lesssim 10^{-3}$. Therefore the two types of experiment are about equally sensitive as tests of μ-e-γ interactions, but the former has a simpler dependence on the form of the interaction.

The authors would like to thank Dr. D. Berley, Dr. J. Lee, Dr. R. Serber, and Dr. J. Weneser for helpful discussions.

---

*This work was supported in part by the U. S. Atomic Energy Commission.

†Now at the Lawrence Radiation Laboratory, Berkeley, California.

‡Now at the Department of Physics, Columbia University, New York, New York.

[1] See J. Schwinger, Ann. Phys. 2, 407 (1957) for a possible alternative to this conclusion.

[2] G. Feinberg, Phys. Rev. 110, 1482 (1958).

[3] Davis, Roberts, and Zipf, Phys. Rev. Letters 2, 211 (1959); and Berley, Lee, and Bardon, Phys. Rev. Letters 2, 357 (1959).

[4] See however, M. Ebel and F. J. Ernst (to be published).

[5] We use Dirac matrices γ_μ satisfying $\{\gamma_\mu, \gamma_\nu\} = 2g_{\mu\nu}$ ($\mu = 0, 1, 2, 3$), $\gamma_5 = i\gamma_0\gamma_1\gamma_2\gamma_3$, and $\sigma_{\mu\nu} = (1/2i)[\gamma_\mu, \gamma_\nu]$. The spinors are normalized by $\bar{u}u = m/E$.

[6] Such an interaction with $f = \mu$ has been discussed by Gamba, Marshak, and Okubo (to be published) who conclude that it cannot be present in strength equal to the Fermi coupling because it generates $\mu \to 3e$ by the mechanism we discuss. We thank Dr. Marshak for a discussion on this point.

[7] J. M. Jauch and F. Rohrlich, The Theory of Photons and Electrons (Addison-Wesley Press, Cambridge, 1955), p. 194.

[8] After this work was done, we received a communication from Dr. T. Kinoshita discussing the μ-e transition in a Coulomb field by this mechanism. His conclusions are quite similar to ours. We thank Dr. Kinoshita for his communication. See also S. P. Rosen (to be published) who also discusses the μ-e transition in a Coulomb field, through the μ-e-γ interaction.

[9] We are indebted to Dr. Juliet Lee for a discussion of the relevant experimental problems.

[10] R. Hofstadter, Revs. Modern Phys. 28, 214 (1956).

[11] R. Gatto, Nuovo cimento, 10, 1559 (1953).

[12] J. Steinberger and H. Wolfe, Phys. Rev. 100, 1480 (1955).

[13] N. M. Kroll and W. Wada, Phys. Rev. 98, 1355 (1955).

[14] N. Samios and J. Lee (to be published).

ABSTRACTS

In this section are printed the abstracts of Articles that have been forwarded to The American Institute of Physics for publication in THE PHYSICAL REVIEW. In quoting information obtained from this section before the appearance of the corresponding Article, reference should be made to "Physical Review (to be published)" rather than to this Journal.

ROLE OF FUSION CHAIN REACTIONS IN THE NONSTATIONARY EVOLUTION OF STARS – SUPERNOVA STARS. M. Gryzinski, Institute of Nuclear Research, Polish Academy of Science, Warsaw, Poland (Received November 13, 1958; revised manuscript received May 20, 1959).

The hypothesis is suggested that the cause of the explosion of supernova stars is the development of a fusion chain reaction in stellar material containing a large amount of He^3 at high densities, $\sim 2\times10^4$ g/cc. It is suggested that the conditions suitable for a strong concentration of He^3 exist only for relatively small hydrogen stars. The strength of the explosion is proportional to the amount of He^3 amassed which strongly depends on the mass of the star. The proto-stars with masses smaller than the mass of the sun lead to supernovae of type I and the proto-stars with masses equal or greater than the mass of the sun lead to supernovae of type II. The remnant of a supernova of type I is the gaseous nebula of luminosity due to the decay of Be^7 created during the explosion in the reaction $He^4(He^3, \gamma)Be^7$.

DISSIPATION OF CURRENTS IN IONIZED MEDIA. O. Buneman,* Stanford University, Stanford, California (Received February 6, 1959).

The destruction of electron drifts by instabilities is analyzed. The fastest stable drift is calculated (drift energy $0.9kT$) and the energy of a faster drift is found to be dissipated into instabilities within, typically, 30 plasma periods. The growth of a local disturbance in this process is shown to take place without effective propagation. The "turbulent" flow pattern created, eventually, under nonlinear conditions is calculated numerically, demonstrating the tendency towards randomization of the initial drift energy. The effect stops "runaway" in about 100 plasma periods after which there is "heating" by "collective collisions" instead.

*Now at Peterhouse, Cambridge, England.

ELECTRON AND ION RUN-AWAY IN A FULLY IONIZED GAS. H. Dreicer, University of California; Los Alamos Scientific Laboratory, Los Alamos, New Mexico (Received February 13, 1959).

Hydrodynamic equations are used to describe the flow of the electrons and ions of a fully ionized gas under the action of an electric field, $\vec{E}$, of arbitrary magnitude. The dynamical friction force exerted by the electrons and ions upon each other through the agency of two-body Coulomb encounters is evaluated. In this connection the electrons and ions have been assigned Maxwellian velocity distributions which are displaced from each other by their relative drift velocity. This treatment yields a dynamical friction force which maximizes when the relative drift velocity is equal to the sum of the most probable random electron and ion speeds. For relative drift velocities in excess of this value the friction force decreases rapidly. As a consequence, it is found that a fully ionized gas cannot exhibit the steady-state behavior characterized by time-independent drift velocities which has previously been accredited to it by other authors. Instead, it is shown that the electron and ion currents flowing parallel to the existing magnetic fields increase steadily in time (i.e., run-away) as long as a component of the electric field along the magnetic field persists. Drift velocities which greatly exceed the random speeds of the plasma particles can be created in this manner.

The theory yields a critical electric field parameter, E_c, which is proportional to the plasma density and inversely proportional to its temperature. It is a measure of the electric field which is required if the drift velocities are to increase and exceed the most probable random speeds in the gas in one mean free collision time. For electric fields in excess of E_c, run-away proceeds even faster. In smaller fields, run-away occurs when Joule heating has depressed E_c sufficiently. Several interpretations of E_c are given in terms of the collisional phenomenon involved.

Within the framework of the hydrodynamic

equations it is shown that the well-known (temperature)$^{3/2}$ electrical conductivity law can be recovered, provided $E \ll E_C$ and the electron temperature is held constant.

Numerical solutions giving electron temperature and drift velocity as a function of time are presented for a range of the ratio E/E_C. The assumption of the displaced Maxwellian distribution is justified on the basis of a comparison between the rate of Joule heating and the rate of equipartition of random speeds. Moreover, it is found that the use of an anisotropic velocity distribution does not affect the run-away phenomenon in any important way.

The possibility of run-away induced across magnetic fields by steep pressure gradients and its relation to diffusion across magnetic fields is examined and discussed in detail.

ELECTRON DAMAGE THRESHOLDS IN InSb. F. H. Eisen and P. W. Bickel, Atomics International, Division of North American Aviation, Incorporated, Canoga Park, California (Received February 18, 1959).

Measurements of carrier removal rate and isochronal recovery in electron-irradiated InSb indicate that displacements are produced at electron energies as low as 240 kev. Two recovery stages have been found and the activation energies for recovery determined. The conductivity recovery in the low-temperature stage was found to be first-order.

RECOMBINATION PROPERTIES OF NICKEL IN GERMANIUM. G. K. Wertheim, Bell Telephone Laboratories, Murray Hill, New Jersey (Received February 6, 1959).

A study of lifetime in germanium containing nickel impurities has shown that the recombination process must be interpreted in terms of a multilevel model, with three charge states assigned to nickel. At room temperature the electron-capture cross section of neutral nickel is 0.96×10^{-16} cm^2, and that of singly negative nickel is 5.9×10^{-16} cm^2; the capture constants in both cases are independent of temperature. The cross section of doubly negative nickel for holes is approximately 1×10^{-14} cm^2; no information on the temperature dependence of this cross section has been obtained. Lifetime data are in good agreement with the known energy levels and solid solubility. The results are compared with those in the literature.

PARAMAGNETIC RELAXATION IN NICKEL FLUOSILICATE. K. D. Bowers and W. B. Mims, Bell Telephone Laboratories, Murray Hill, New Jersey (Received February 17, 1959).

Physical models of the paramagnetic relaxation process are briefly reviewed, and a description is given of the pulsed-microwave method of investigation. This method has been applied to the study at low temperatures of zinc/nickel fluosilicate at various magnetic dilutions, and an additional relaxation process has been observed which is associated with the sharing of energy among the spins.

The results depend only on the temperature and magnetic concentration, and are independent of all other experimental conditions provided that excessive power levels are avoided. The lack of size dependence indicates that the relaxation rate is not controlled by spatial diffusion of phonons. The temperature dependence which has been observed is too acute to fit the $1/T$ law of the simple "direct process" model, and suggests that the relaxation rate is controlled either by phonon combination probabilities or by a Raman type of interaction between phonons and spins.

ELASTIC CONSTANTS OF α-BRASSES: VARIATION WITH SOLUTE CONCENTRATION FROM 4.2 TO 300°K. J. A. Rayne, Westinghouse Electric Corporation, Pittsburgh, Pennsylvania (Received February 6, 1959).

Elastic-constant measurements have been made on a representative series of α-brasses in the temperature range 4.2-300°K. No appreciable change with temperature occurs in the dependence of C and C' on solute concentration. Possible explanations for this result are considered. The Θ values for the alloys, as computed for the elastic-constant data at 4.2°K, differ significantly from the calorimetric values. It is believed that this discrepancy results from the difference between the phonon wavelengths used in the ultrasonic measurements and those contributing to the lattice heat capacity of the alloys at low temperatures.

ANTIFERROMAGNETIC STRUCTURES OF MnS_2, $MnSe_2$, and $MnTe_2$. J. M. Hastings, N. Elliott, and L. M. Corliss, Chemistry Department, Brookhaven National Laboratory, Upton, New York (Received February 13, 1959).

The antiferromagnetic structures of MnS_2, $MnSe_2$, and $MnTe_2$ have been obtained by neutron diffraction. The disulfide exhibits ordering of the "third" kind, the ditelluride, ordering of the "first" kind, and the diselenide, an arrangement which is intermediate between the two. The structures are discussed from the viewpoint of indirect exchange. Magnetic susceptibilities, obtained by the Gouy method, are reported for all three compounds.

ELECTRON PARAMAGNETIC RESONANCE IN $SrTiO_3$. W. L. Dobrov, R. F. Vieth, and M. E. Browne, Lockheed Research Laboratories, Palo Alto, California (Received February 13, 1959).

The intensities of paramagnetic resonance lines in $SrTiO_3$ have been correlated to the iron concentrations. Evidence for attributing the origin of the resonance in titanates to iron impurities (Fe^{3+}) rather than to the domain structure was obtained. In $SrTiO_3$, resonance experiments over the temperature range 300°K to 1.9°K show a slow continuous increase of the tetragonal component of the crystalline field down to the ferroelectric region. From intensity considerations the absolute signs of the crystalline splitting parameters have been determined.

ENERGY DEPENDENCE OF RECOVERY IN IRRADIATED COPPER. J. W. Corbett and R. M. Walker, General Electric Research Laboratory, Schenectady, New York (Received February 9, 1959).

Stage I recovery (10°K-65°K) in electron-irradiated copper consists of five substages of recovery, designated as $I_A - I_E$ in order of increasing temperature. We report here the shift in the populations of $I_A - I_E$ as a function of the energy of the bombarding electrons. The sum of the first three substages (I_A, I_B, and I_C) increases with decreasing bombarding energy at the expense of the higher temperature substages. The ratio I_D/I_E also increases with decreasing energy. The data are interpreted as corroboration of a previously proposed model for stage I recovery. The measured shifts are quite small. This is discussed in relation to the recoil energy distributions and it is concluded that the most likely interpretation is that the average separation between a primary recoil and its vacancy does not vary rapidly with increasing recoil energy near threshold. Several possible explanations for this behavior are outlined.

X-RAY MEASUREMENT OF THE ATOMIC SCATTERING FACTOR OF IRON. Boris W. Batterman,* Bell Telephone Laboratories, Murray Hill, New Jersey (Received February 11, 1959).

The x-ray integrated intensities of Bragg reflections of iron, copper, and NaCl powders were measured with monochromatic Fe K_α radiation. By investigating the effect of cold work on intensities of the metal powders and comparing the measured intensities of different orders with theoretical values, it was shown that extinction, surface roughness, and preferred orientation effects were negligible. The four measured iron reflections gave atomic scattering factors relative to either copper or NaCl which agreed, within experimental error, with values calculated from wave functions of the isolated iron atom. It is estimated that the experimental form factor for the lowest order reflection of copper and iron agrees with free atom values to an error corresponding to the contribution of ±one free-atom-3*d* electron. This is to be contrasted with results of Weiss and DeMarco, who concluded from single-crystal measurements that metallic iron has (2.3 ± 0.3) 3*d* electrons, compared with 6 for the free atom.

*Present address: IBM Research Laboratory, Poughkeepsie, New York.

K ABSORPTION EDGE OF SELENIUM. Richard D. Deslattes* and Hillery S. deBen, Florida State University, Tallahassee, Florida (Received February 9, 1959).

Use of thin unsupported selenium absorbers has permitted observation of significant structure in the *K* absorption spectrum. Observations of the $K\beta_2$ emission and the fundamental optical absorption of similar samples have been made and used to assist in the interpretation of the

K-edge structure. It is suggested that the prominent absorption maximum at the experimentally determined "edge" arises from transitions to an x-ray excitation state or states in the region of the forbidden energy gap. The following general absorption is attributed to transitions to the conduction band. The gap energy required in this interpretation is approximately 4 electron volts, indicating that the lower part of the conduction band contains little p-type symmetry.

*Present address: Cornell University, Ithaca, New York.

MAGNETIC SUSCEPTIBILITY OF CLOSE-PACKED HEXAGONAL GOLD-INDIUM ALLOYS. T. B. Massalski,* Department of Physical Metallurgy, The University, Birmingham, England, and L. Meyer and D. Weiner, Institute for the Study of Metals, The University of Chicago, Chicago, Illinois (Received February 16, 1959).

The magnetic susceptibility of close-packed hexagonal gold-indium alloys has been measured at 300°K, 77°K, 4.2°K, and 1.2°K. The susceptibility data show a striking similarity to the c-axis spacing exhibiting a maximum at about 19 atom % In, consistent with a model assuming that the Fermi surfaces touch the Brillouin zone face (0002) at this concentration.

*Now at Mellon Institute, Pittsburgh, Pennsylvania.

APPROACH TO BOLTZMANN EQUILIBRIUM OF THE NUCLEAR SPINS IN A QUADRUPOLAR SOLID. Walter I. Goldburg, Carnegie Institute of Technology, Pittsburgh, Pennsylvania (Received August 21, 1958; revised manuscript received April 1, 1959).

A single crystal of $NaNO_3$ is oriented in an external magnetic field at an angle (θ_1) for which the quadrupole splitting is large. With radio-frequency radiation, a pair of Zeeman levels of the sodium nuclear spin system ($I = \frac{3}{2}$) is saturated. Then the crystal is quickly rotated to an angle where the inequality of the level spacings is a minimum (approximately $\frac{1}{2}$ the line width) and where spin mixing can take place. The crystal is then quickly returned to θ_1 where, by nuclear resonance pulse techniques, the populations of the four sodium levels can be determined. This sequence of operations is completed in a time short compared to the spin lattice relaxation time. When the $m = \pm\frac{1}{2}$ levels are initially saturated, the spin system rapidly comes to the expected spin temperature, $T_S = \frac{1}{3}\theta$ the lattice temperature. When the outer satellites are saturated, however, the resulting equilibrium populations of the levels are not those of a Boltzmann distribution. Also measured was the rate of approach of the spin system to equilibrium for various larger splittings. For splittings of the order of the line width, an unexpected plateau appears in the spin mixing rate. The usual rate equations do not seem adequate to describe the observed dynamic behavior of this spin system.

HARTREE-FOCK THEORY WITH NONORTHOGONAL BASIS FUNCTIONS. R. McWeeny, Departments of Mathematics, Physics and Chemistry, University College of North Staffordshire, Staffordshire, England (Received January 19, 1959).

Solutions of the Hartree-Fock self-consistent-field equations can be approximated by linear combination of a set of basis functions: the equations then assume a matrix form, as shown by Roothaan. It is possible, however, to obtain the required variational solution of the many-electron problem much more directly by an iterative construction of the density matrix. This method, first developed by the author for expansion in terms of orthogonal basis functions, is extended to the case of a nonorthogonal set.

GROUND STATE OF THE HELIUM ATOM. II. Toichiro Kinoshita,* Bell Telephone Laboratories, Murray Hill, New Jersey, and Laboratory of Nuclear Studies, Cornell University, Ithaca, New York (Received February 19, 1959).

A further attempt is made to improve the theoretical prediction of the energy of the ground state of atomic helium. The nonrelativistic part is treated by the variational method of Stevenson and Crawford which is useful for improving the lower bound for the ground state energy. Linear combinations of up to 80 terms of generalized Hylleraas type are employed in the numerical computation. The best trial function gives -2.9037237 as an upper bound and -2.9037467 as a lower bound for the ground state energy. It is estimated from the calculated results that the

exact nonrelativistic energy of He ground state will be found in the neighborhood of -2.9037247. Rigorous formulas are derived which can be used for calculating the upper limits to the errors in the expectation values of mass polarization and relativistic corrections. Although these formulas give very broad limits of error, they are useful in estimating the order of magnitude of actual errors in a semiempirical manner. With mass polarization and relativistic corrections as well as electrodynamical corrections, the theoretical ionization potential becomes 198 310.76 cm^{-1} which is in good agreement with the latest observed value $198\,310.8_2 \pm 0.15$ cm^{-1}.

*Permanent address: Cornell University, Ithaca, New York.

L TO *K* ELECTRON CAPTURE RATIO IN Ge^{71}. D. E. Rehfuss* and Bernd Crasemann, Department of Physics, University of Oregon, Eugene, Oregon (Received July 25, 1958).

By comparison of the number of 0.175-Mev gamma rays occurring in the decay of As^{71} with the number of gallium *K* x-rays proceeding from Ge^{71} *K* capture, the relative amount of *L* capture in Ge^{71} has been determined indirectly. Solid sources and a scintillation spectrometer were employed. The Ge^{71} *L*/*K* electron capture ratio is found to be 0.09 ± 0.05, in agreement with theory.

*Now at the Los Alamos Scientific Laboratory of the University of California, Los Alamos, New Mexico.

NEUTRON-PROTON CAPTURE CROSS SECTION. Robert W. Stooksberry and Marshall F. Crouch, Case Institute of Technology, Cleveland, Ohio (Received January 28, 1959).

The mean lifetime of thermal neutrons in water is measured with a large moderator (radius ~ 7 diffusion lengths), for which the correction for escape is only about 5%. The geometry is such that the perturbing effect of the immersed BF_3 neutron detector can be almost rigorously calculated. The value obtained is $\tau = 206.3 \pm 5.0$ μsec, giving the neutron-proton capture cross section as $(0.330 \pm 0.008) \times 10^{-24}$ cm^2. A possible systematic error from higher modes in the neutron distribution is discussed.

INVESTIGATIONS OF THE $Be^9(p,n)B^9$ and $Be^9(p,\alpha\gamma)Li^6$ REACTIONS. Jerry B. Marion, Los Alamos Scientific Laboratory, Los Alamos, New Mexico, and University of Maryland, College Park, Maryland, and Jules S. Levin, Los Alamos Scientific Laboratory, Los Alamos, New Mexico (Received February 12, 1959).

A pulsed-beam time-of-flight technique has been used to study neutrons and γ rays from the proton bombardment of Be^9 in the energy range from 2.3 to 5.4 Mev. Excitation curves for the ground-state neutron group from the $Be^9(p,n)B^9$ reaction have been measured at 0° and 90°. These curves show the well-known resonances at 2.56 and 4.6 Mev and, in addition, show a broad maximum near 3.5 Mev. The γ-ray excitation curve also indicates maxima at 2.56, 3.5, and 4.5 Mev. The 3.5- and 4.6-Mev resonances are tentatively assigned to *p*- and *d*-wave states having $(J = 2^+, T = 1)$ and $(J = 3^-, T = 1)$, respectively. The previously observed maximum near 4.9 Mev appears to be the result of the effect of the 3.5-Mev resonance on the n_1 group immediately above its threshold. The cross section for the production of continuum neutrons is appreciable for proton energies above about 3 Mev. A large fraction of these neutrons appears to result from the neutron decay of the 2.43-Mev Be^9 level following the inelastic excitation of this level.

NUCLEAR SPECTROSCOPIC STUDIES OF NEUTRON-DEFICIENT ISOTOPES IN THE RARE EARTH REGION. Kenneth S. Toth* and John O. Rasmussen, Radiation Laboratory and Department of Chemistry, University of California, Berkeley, California (Received November 3, 1958).

The conversion-electron spectra of four neutron-deficient rare earth isotopes are presented and discussed. The four isotopes are Tb^{153}, Tb^{154}, Dy^{155}, and Ho^{160}. Mihelich, Harmatz, and Handley in a recent publication have presented the conversion-electron data of a large number of rare earth isotopes, including all but one (Dy^{155}) of the four above-mentioned activities. The agreement between the two works is good. Some additional conversion lines, not reported by Mihelich et al., have been identified in this work as belonging to the decay of Tb^{153}, Tb^{154}, and Ho^{160}. Decay schemes are proposed for

Dy^{155} and Tb^{153}. Tb^{154} and Ho^{160} decay to levels in Gd^{154} and Dy^{160}, respectively. The electron-capture decay data of Tb^{154} and Ho^{160} are compared with data obtained by other workers in the negatron decay of Eu^{154} and Tb^{160} to levels in Gd^{154} and Dy^{160}, respectively, and transitions common to both modes of decay are noted.

*Present address: University Institute for Theoretical Physics, Copenhagen, Denmark.

NEW TERBIUM ISOTOPE, Tb^{152}. Kenneth S. Toth,* Kenneth T. Faler, and John O. Rasmussen, Radiation Laboratory and Department of Chemistry, University of California, Berkeley, California (Received November 6, 1958).

A careful examination of photon and electron spectra from cyclotron-produced mixtures of light terbium isotopes has led to the indentification of a new isotope, Tb^{152}, with an 18.5-hr half-life. The 344.1-kev transition from first excited state to ground in daughter Gd^{152} has been identified and shown to be identical in energy to a transition associated with the beta decay of 9.3-hr Eu^{152m} to the same daughter nucleus. Gamma transitions of 180 and 265 kev are also assigned to the decay of Tb^{152}.

*Present address: University Institute for Theoretical Physics, Copenhagen, Denmark.

BETA DECAY OF Bk^{250} AND Bk^{249}. Susanne E. Vandenbosch, Herbert Diamond, Ruth K. Sjoblom, and Paul R. Fields, Argonne National Laboratory, Lemont, Illinois (Received February 4, 1959).

The beta decay of Bk^{250} has been studied with a beta spectrometer. Bk^{250} has two beta groups: 725 ± 15 kev (89 ± 1% abundant) and 1760 ± 50 kev (11 ± 1% abundant). Conversion electron lines corresponding to 42.2, 98.2, 890, 930, 990, and 1032-kev transitions were observed and their intensities measured. The information obtained from crystal spectrometer singles and coincidence measurements was combined with beta spectrometer data to construct a decay scheme for Bk^{250} involving gamma vibrational levels in Cf^{250} analogous to those found in Pu^{238}. The beta half-life of Bk^{250} is 193.3 ± 0.3 minutes. The electron-capture partial half-life of Bk^{250} is estimated to be greater than 5 years. The beta spectrum of Bk^{249} shows an allowed or first forbidden transition with an end-point energy of 125 ± 2 kev.

METASTABILITY OF PLATINUM-199. Morris A. Wahlgren and W. Wayne Meinke, Department of Chemistry, University of Michigan, Ann Arbor, Michigan (Received February 12, 1959).

A metastable state of platinum-199 has been produced by thermal neutron irradiation of normal and enriched platinum samples. The isomer decays with a half-life of 14.1 ± 0.3 seconds by the emission of γ rays of 32 ± 2 and 393 ± 2 kev energy. The thermal neutron activation cross section of Pt^{198} for the formation of the isomer is 0.028 ± 0.003 barn. Tentative level assignments are made, consistent with systematics and shell theory.

ANGULAR DISTRIBUTIONS OF NEUTRONS INELASTICALLY SCATTERED FROM SODIUM. E. N. Shipley,* G. E. Owen, and L. Madansky, Physics Department, The Johns Hopkins University, Baltimore, Maryland (Received February 6, 1959).

The angular distribution and total cross section for inelastic neutron scattering proceeding to the first excited state in sodium have been measured by observing the neutron-gamma coincidences. The measured total cross sections for the various neutron energies used are $\sigma_T(3.49\ \text{Mev}) = 370 \pm 120$ mb, $\sigma_T(3.75\ \text{Mev}) = 270 \pm 90$ mb, and $\sigma_T(4.00\ \text{Mev}) = 280 \pm 90$ mb. The differential cross sections were found to be higher in the backward than in the forward directions.

*Now at Physics Department, Northwestern University, Evanston, Illinois.

DECAY OF SHORT-LIVED BARIUM AND LANTHANUM FISSION PRODUCTS. R. P. Schuman, E. H. Turk, and R. L. Heath, Phillips Petroleum Company, Atomic Energy Division, Idaho Falls, Idaho (Received February 13, 1959).

The half-lives and gamma spectra of the short-lived barium and lanthanum fission products have been measured. Ba^{141} has a half-life of 18 ± 1 min and emits x-rays and gamma rays of

120 kev, 190 kev, 290 kev, ~350 kev, 460 kev, 640 kev, and 740 kev. Ba^{142} has a half-life of 11±1 min and emits x-rays and gamma rays of 80 kev, ~260 kev, 890 kev, 970 kev, 1080 kev, 1200 kev, 1360 kev, and 1680 kev. La^{141} has a half-life of 3.85±0.10 hr and emits a low-intensity gamma ray at 1370 kev. La^{142} has a half-life of 85±6 min and emits gamma rays of 640, 900, 1030, 1080, 1370, 1540, 1750, 1920, 2080, 2400, 2570, 3000, 3300, and 3650 kev.

STATISTICS OF SLOW-NEUTRON "NEGATIVE" ENERGY RESONANCES. P. A. Egelstaff, Atomic Energy of Canada Limited, Chalk River, Ontario, Canada (Received February 9, 1959).

Neutron cross sections measured with very slow neutrons often reveal the influence of levels below the neutron binding energy. The published data on 20 isotopes are analyzed in such a way that the properties of the levels below and above the binding energy may be compared. It is found, in particular, that the neutron width and level spacing distributions for these (- and +) levels are the same within the limits of the present analysis.

DECAY OF K^{43}. N. Benczer-Koller, A. Schwarzschild, and C. S. Wu, Columbia University, New York, New York (Received January 2, 1959).

The decay of K^{43} has been reinvestigated in an attempt to clarify the discrepancies existing in the ordering of the energy levels of Ca^{43}. The external conversion spectrum showed lines corresponding to the following gamma-ray energies: 0.220±0.002, 0.371±0.002, 0.388±0.002, 0.394 ±0.002, 0.591±0.003, 0.614±0.004 Mev. In addition a γ ray of 1.005 Mev was observed in the scintillation spectrum. β-γ coincidence measurements establish that the gamma transitions to the ground state are the 0.371-Mev and the 0.591-Mev gamma rays and not the 0.614-Mev gamma ray as believed previously. These results and the γ-γ coincidence measurements indicate only one possible level scheme in Ca^{43}: 0, 0.371, 0.591, 0.985, 1.373 Mev. These energy levels as well as their proposed spin and parity assignments are in good agreement with the results from the MIT nuclear reaction data. A two-cycle baffle for the solenoid β spectrometer is described. This baffle reduces significantly the background due to scattered gamma radiation from very strong external conversion sources.

RANGE-ENERGY RELATIONS FOR PROTONS IN Be, C, Al, Cu, Pb, AND AIR. R. M. Sternheimer, Brookhaven National Laboratory, Upton, New York (Received February 6, 1959).

Range-energy relations for protons have been obtained for six substances (Be, C, Al, Cu, Pb, and air). The calculations for the energy loss dE/dx include the shell corrections at low energies, and the density effect which becomes important in the high-energy region. The present results can also be used to determine the range of μ mesons up to ~10 Bev. Besides the calculated values of the range, tables of the ionization loss dE/dx are also presented.

INTERACTION OF YTTRIUM WITH PROTONS OF ENERGY BETWEEN 60 AND 240 Mev. Albert A. Caretto, Jr.,* and Edwin O. Wiig, Department of Chemistry, University of Rochester, Rochester, New York (Received October 24, 1957; revised manuscript received March 30, 1959).

Absolute cross sections are reported for a number of nuclides produced by the interaction with yttrium of protons of 60, 100, 150, 180, and 240 Mev. At low energies the yields can be accounted for by direct interaction or knock-on processes. At higher energies the knock-on cascade model together with evaporation appears to explain the observed yields.

*Present address: Lawrence Radiation Laboratory, Livermore, California.

γ-γ ANGULAR CORRELATION MEASUREMENTS OF THERMAL NEUTRON CAPTURE γ-RAYS IN MAGNESIUM, SILICON, PHOSPHORUS, AND SULFUR. G. Manning * and G. A. Bartholomew, Atomic Energy of Canada Limited, Chalk River, Ontario, Canada (Received February 16, 1959).

A description is given of an angular correlation apparatus, using two NaI(Tl) scintillation spectrometers, which has been used to study cascades of γ-radiation following thermal neutron capture. The elements studied were magnesium,

silicon, phosphorus, and sulfur. The following new spin assignments were made: the 4.93-Mev level of Si^{29}, 3/2; 6.38-Mev level of Si^{29}, 1/2; 1.15-Mev level of P^{32}, 1; and 3.26-Mev level of P^{32}, 2. In addition, the spins of the 3.41-Mev level of Mg^{25} and the 3.22-Mev level of S^{33} have been confirmed to be 3/2. Other aspects of the decay schemes are discussed.

*Present address: Norman Bridge Laboratory of Physics, California Institute of Technology, Pasadena, California.

$Li^6(n,t)He^4$ REACTION AT INTERMEDIATE ENERGIES. S. J. Bame, Jr., and R. L. Cubitt, Los Alamos Scientific Laboratory, University of California, Los Alamos, New Mexico (Received November 6, 1958).

The $Li^6(n,t)He^4$ reaction cross section has been measured in a neutron energy interval extending from 9 kev to 340 kev. The cross section descends from 1.77 barns at 9 kev to a minimum of 0.74 b at 100 kev before rising to a peak resonance value of 2.75 barns at 258 kev. The cross section from 9 kev to 90 kev is not proportional to $E^{-1/2}$, but can be represented by $\sigma = 3.96E^{-0.367}$ with σ in barns and the neutron energy E in kev. Angular distributions of the tritons are presented for neutron energies of 150, 200, 258, 300, 350, and 565 kev. These distributions, measured in a relative manner, are placed on an absolute scale by normalizing to the cross-section data of this experiment, extended to 565 kev by use of previously measured cross sections.

DIFFERENTIAL CROSS SECTIONS OF SOME (α,p) REACTIONS. C. E. Hunting* and N. S. Wall, Department of Physics and Laboratory for Nuclear Science, Massachusetts Institute of Technology, Cambridge, Massachusetts (Received February 16, 1959).

Using 30.4-Mev alpha particles, proton differential cross sections have been obtained for the following transitions, corresponding to discrete states of the residual nuclei: $B^{10}(\alpha,p)C^{13}$ gnd; $Na^{23}(\alpha,p)Mg^{26}$ gnd, 1.83 Mev; $P^{31}(\alpha,p)S^{34}$ gnd; and $Al^{27}(\alpha,p)Si^{30}$ gnd, 2.24 Mev. A proton energy spectrum corresponding to the first 12 Mev of excitation of the residual nucleus was obtained for the case involving the Al^{27} target. The differential cross sections are interpreted with the aid of predictions of the Butler direct interaction (surface) theory. It is concluded that this theory is probably a more useful tool in interpreting the results obtained than is the compound nucleus theory. Some deviations from the predictions of the surface direct-interaction calculations are discussed.

*Now at the Oak Ridge National Laboratory, Oak Ridge, Tennessee.

ENERGY LEVELS IN Na^{23} FROM THE $Ne^{22}(p,\gamma)Na^{23}$ REACTION. J. J. Singh, V. W. Davis,* and R. W. Krone, Department of Physics, University of Kansas, Lawrence, Kansas (Received January 26, 1959).

The gamma-ray excitation function for the $Ne^{22}(p,\gamma)$ reaction has been investigated in the energy range of 600 kev to 1800 kev. Eleven resonances could definitely be identified as resulting from this reaction. The cascades leading to the ground state of Na^{23} were determined and found to proceed for the most part through well-known lower lying states, although no gamma rays corresponding to transitions through the 2.08-Mev and 2.39-Mev states were observed at any of the resonances investigated.

*Now at Los Alamos Scientific Laboratory, Los Alamos, New Mexico.

DISPERSIVE EFFECTS IN ELECTRON-NUCLEUS INTERACTIONS. Nicholas A. Krall* and E. E. Salpeter, Laboratory of Nuclear Studies, Cornell University, Ithaca, New York (Received February 16, 1959).

Elastic scattering of electrons from nuclei is influenced by the possibility of virtual transitions to excited nuclear states in intermediate states. Such dispersive corrections to elastic electron-deuteron scattering are calculated in second order Born approximation for incident electron energies from 200 Mev to 500 Mev for various values of the momentum transfer. The static second order Born formulas are also evaluated. Similar, but less accurate, calculations are carried out for He^4, C^{12}, and some heavier elements. These results are used to find small corrections to nuclear radii obtained from an analysis of the Stanford experiments.

Dispersive effects on the energy-level shifts in bound s-states of hydrogenic atoms are also calculated, using second order perturbation theory for the deviation of the nuclear charge distribution from a point charge. These small shifts are evaluated for deuterium and He and, less accurately, for other nuclei with $Z < 50$.

*Now at the John Jay Hopkins Laboratory for Pure and Applied Science, General Atomic Corporation, San Diego, California.

GEOMETRY OF GRAVITATION AND ELECTROMAGNETISM. Louis Witten, RIAS, Baltimore, Maryland (Received January 21, 1959).

An independent derivation is given of equations first derived by Rainich which show how, under certain circumstances, the combined theory of gravitation and electromagnetism of Einstein and Maxwell can be unified and described exclusively in terms of geometry. Some algebraic relations are presented between the Ricci tensor, the electromagnetic field tensor, and their principal null vectors. It is shown that in regions of space-time where the two invariants of the electromagnetic field both vanish, the unified theory cannot apply. Either such regions do not exist in nature or their description in terms of pure geometry has yet to be found. Advantage is taken of the correspondences between tensors and spinors to carry out most of the present calculations in spinor space.

PHENOMENOLOGICAL ANALYSIS OF HYPERON DECAY. S. A. Bludman, Lawrence Radiation Laboratory, University of California, Berkeley, California (Received February 16, 1959).

The $\Delta I = \frac{1}{2}$ rule is incorporated into a previously discussed universal weak Yukawa interaction by assuming the simplest relation between chirality and charge operators. Expressing the $\Delta I = \frac{1}{2}$ rule by forming the π and Ξ isospinors into an isovector $\vec{B}$ and an isoscalar B_0, we assume that $\vec{B}$ occurs (as in β decay) with $g\gamma_\mu(\frac{1}{2}+\frac{1}{2}r\gamma_5)$ and B_0 (which has no β-decay counterpart) with $g\gamma_\mu(\frac{1}{2}-\frac{1}{2}r\gamma_5)$. Here g is the constant previously fitted to the π decay rate, and r the ratio of Gamow-Teller and Fermi coupling constants. Depending on the sign taken between the $\vec{B}$ and B_0 interaction terms, Σ decays into $n+\pi^+$ in pure S and into $p+\pi^-$ in pure P channels, or vice versa. In either case, $\Sigma^+ \to p+\pi^0$ involves maximal S-P interference and $\alpha^0 = 0.98$. Decay into $I = \frac{1}{2}$ proceeds via $\gamma_\mu(\frac{1}{2}+\frac{3}{2}r\gamma_5)$ or $\gamma_\mu(\frac{3}{2}+\frac{1}{2}r\gamma_5)$, depending on whether Σ decay is pure S or pure P. The second case, but not the first, leads to a Λ decay rate in agreement with experiment. In this case $\alpha_\Lambda = 0.54$; and in Ξ decay, $\alpha_\Xi = 0.64$ and the calculated decay rate is 2.4×10^{-10} sec^{-1}.

INTERFERENCE EFFECTS IN LEPTONIC DECAYS. Steven Weinberg, Columbia University, New York, New York (Received February 17, 1959).

It is proven that in a leptonic decay experiment in which the lepton masses and charges may be neglected, and in which no pseudoscalar correlations are measured, all VA interference terms will be antisymmetric under exchange of the two leptons, while the pure V and A terms will be symmetric. If the experiment measures a pseudoscalar correlation, these conclusions are reversed. Even if the lepton masses cannot be ignored (e.g., for $\Lambda^0 \to \mu^- + \bar{\nu} + p$, or low-energy β decay), it is still true that no VA interference may appear when scalars are measured, and only VA interference may contribute when pseudoscalars are measured, providing that the lepton spins and momenta are not directly observed. Thus experiments can be devised that involve no interference effects, or only interference effects. This theorem holds independently of the strangeness change, spin change, energy transfer, or of any particular assumptions about the form of the V and A currents. It proves most useful when it is difficult or tedious to calculate transition rates directly. Applications are discussed, including possible tests of the Feynman–Gell-Mann theory in nonunique forbidden β decay, of the nature of the leptonic Λ^0 and K^0 decay interaction, and of the charge symmetry properties of weak interactions.